UTILIZING AN EXTENDED TARGET FOR HIGH FREQUENCY MULTI-BEAM SONAR INTENSITY CALIBRATION

BY

JOHN LANGDON HEATON IV

B.S.M.E/ACOUSTICS, University of Hartford, 2012

THESIS

Submitted to the University of New Hampshire

In Partial Fulfillment of

The Requirements for the Degree of

Master of Science

in

Mechanical Engineering

September, 2014

This thesis has been examined and approved.

_____
Thesis Advisor, Thomas Weber
Assistant Professor of Mechanical Engineering and Ocean Engineering

_____
Kenneth Baldwin, Professor of Mechanical Engineering and Ocean Engineering

_____
Diane Foster, Associate Professor of Mechanical Engineering and Ocean Engineering

_____
Date

DEDICATION

I would like to dedicate this thesis to my wife, Alicia, and my parents, Hilde and John. This effort would not have been completed without your continued support. I sincerely thank you for that.

ACKNOWLEDGEMENTS

I would like to acknowledge the guidance and support provided to me by my research advisor, Dr. Thomas Weber. I would also like to recognize the defense committee, whose comments and suggestions will ultimately serve to improve this work.

Additionally, I would like to thank Carlo Lanzoni, Glen Rice, Briana Welton, and Paul Lavoie of the Center for Coastal and Ocean Mapping/Joint Hydrographic Center for their assistance throughout the course of this project. Further gratitude is due to my fellow CCOM/JHC students, Eric Bajor, Liam Pillsbury, and Kevin Jerram for their help and camaraderie throughout this experience.

TABLE OF CONTENTS

ACKNOWLEDGEMENTS iv
LIST OF FIGURES vi

CHAPTER PAGE

CHAPTER 1 1
1.1 – Introduction 1
CHAPTER 2 5
2.1 – Design and Construction 5
2.2 – Acoustic Characterization of the Extended Target 10
2.3 – Discussion 21
CHAPTER 3 23
3.1 – Introduction 23
3.2 – Calibration Coefficient Development 27
3.3 – MBES Calibration 31
CHAPTER 4 43
4.1 – Field Work with T20-P MBES and EK60 SBES 43
CHAPTER 5 57
5.1 – Conclusions and Remarks 57
LIST OF REFERENCES 62

LIST OF FIGURES

Figure 1.1 – Alongship and Athwartship angles (from Lanzoni [15]) 3
Figure 2.1 – Jack-chain extended target (entire target left, close up right) 8
Figure 2.2 – Acoustic test tank at UNH (from Lanzoni [15]) 9
Figure 2.3 – 3-D EK60 SBES transmit/receive beam pattern (from Lanzoni, personal communication) 10
Figure 2.4 – Positioning of target for angular dependence of *Ss* investigation (left to right, top to bottom) 13
Figure 2.5 – Laser level alignment method with paper target corresponding to calibration target position 14
Figure 2.6 – Beam interaction with target 15
Figure 2.7 – *TS* (left) and *Ss* (right) as a function of incident angle 16
Figure 2.8 – Comparison of the scattered amplitude distribution (blue histogram) with a Rayleigh distribution (red curve) 17
Figure 2.9 – *TS* and *Ss* as a function of range at normal incidence 19
Figure 3.1 – T20-P MBES mounting configuration (receiver top, 200 kHz transmitter bottom) 25
Figure 3.2 – Mills-Cross example beam pattern (single beam, receive left, transmit middle, combined right, from Lanzoni [15]) 26
Figure 3.3 – T20-P saturation measurements, gain vs. *DV* amplitude (dB) for several *SL* settings 32
Figure 3.4 – MBES calibration sweep concept 34
Figure 3.5 – MBES echogram (single ping, midway through calibration sweep) 35
Figure 3.6 – Ping progression with data boundaries of 300 pings (black lines) .. 37
3.7 – Independent realizations of beam 82 38
Figure 3.8 – P value from the KS-test calculated for every beam 39
Figure 3.9 – Calibration curve with 38.1 mm WC sphere comparisons at -45°, 0°, and 45° 41
Figure 4.1 – NEWBEX standard line route, Portsmouth Harbor, Portsmouth, NH 44
Figure 4.2 – Sonar mounting configuration for field deployment 44
Figure 4.3 – Angle dependant backscatter model, 200 kHz 45
Figure 4.4 – T20-P field trial *DV* (dB) 46
Figure 4.5 – Backscatter comparison between EK60 and T20-P beam 82 (steered to -45°, parallel to EK60 MRA), no averaging 48

Figure 4.6 – Averaged backscatter estimates between EK60 and T20-P, 40 ping clusters 49
Figure 4.7 – Zoomed view of field data error estimates 50
4.8 – Linear comparison of seabed backscatter estimates between EK60, T20-P 51
Figure 4.9 – Field data KS-test results 52
Figure 4.10 – Full swath backscatter estimates over certain locations 53
Figure 4.11 – Seabed characterization over clusters 15, 30, 45, 60 from NEWBEX standard line 54
4.12 – Ping cluster locations along the standard NEWBEX survey line 55

LIST OF TABLES

Table 1 – T20-P operational settings summary 32

ABSTRACT

UTILIZING AN EXTENDED TARGET FOR HIGH FREQUENCY MULTI-BEAM SONAR INTENSITY CALIBRATION

BY

JOHN LANGDON HEATON IV

University of New Hampshire, SEPTEMBER, 2014

There exists an interest in expediting intensity calibration procedures for Multi-Beam Echo-Sounders (MBES) to be used for acoustic backscatter measurements. Current calibration methods are time-consuming and complicated, utilizing a target that is different from the seafloor. A target of irregularly oriented chain links arranged in a 'curtain' was constructed to simulate an extended surface, like the seafloor. Tests with a 200-kHz SIMRAD EK60 Split-Beam Echo-Sounder (SBES) to investigate the targets scattering strength were performed. These tests suggest that the scattering strength depends on the number of scattering elements. A 200 kHz Reson SeaBat T20-P MBES was calibrated with the same target. This MBES was rotated so that all beams were

incident on the target. The final output is a beam-dependent calibration coefficient determined from the sonar equation. The T20-P was then used to collect backscatter in the field along a local survey line, where data were compared to the EK60.

CHAPTER 1

CALIBRATED ACOUSTIC BACKSCATTER

1.1 – Introduction

A significant percentage of the world's population lives near the coast and many human endeavors are associated with the seafloor environment [2]. Due to this, there is a requirement for accurate maps of the seabed to maintain and further human oceanographic interests. One way to characterize the seafloor is through collecting calibrated acoustic backscatter. Acoustic backscatter from the seabed is collected for its use in seafloor imaging, seabed mapping, and habitat mapping [17]. This is a topic of great interest because significant knowledge about the structure of the world's oceans can be gained with this information. Acoustic backscatter is often collected with multi-beam echo-sounders (MBES). These systems are used to make measurements of target range and angle, and to gather characteristics of the target based on the intensity of the backscattered signals [17]. Due to the large number of narrow acoustic beams incident on a flat target like the seafloor, it is possible to insonify an immense area with a MBES. MBES systems have become the preferred tool for most ocean mapping research due to this feature. It is necessary to calibrate these systems to collect

accurate acoustic backscatter measurements from the seafloor. The goal of this work is to develop a novel, simple and efficient methodology for calibrating MBES using an extended calibration target that replicates the morphology of the seafloor instead of using the typical reference sphere targets.

Although MBES are widely used, these systems are often not calibrated with regard to backscatter measurements. This may be due to the extensive time required to perform such a calibration using the traditional method. The traditional calibration method for sonar systems utilizes a small (few wavelengths) spherical point target, often a Tungsten Carbide (WC), or Copper sphere (described by Foote, et al [5]). In Foote's method, a reference sphere is incrementally moved through the beam in both the alongship and athwartship directions so that measurements are recorded while the sphere is located on the maximum response axis (MRA) of the beam. This method essentially maps the combined transmit and receive 3-D beam pattern. These reference targets are acoustically characterized [23], and can be used to compute calibration coefficients or beam pattern measurements [14]. The alongship and athwartship geometry is defined in Figure 1.1.

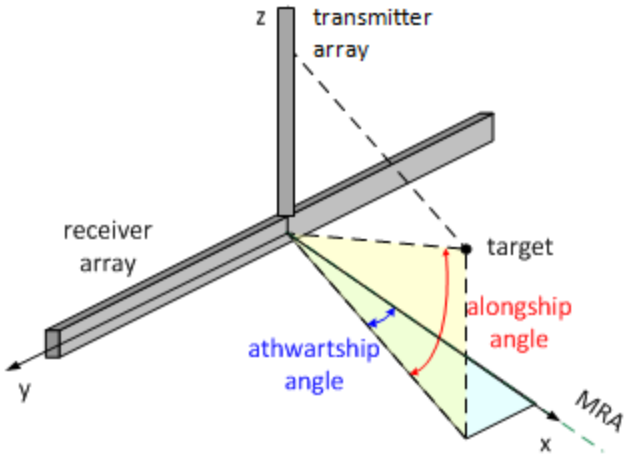

Figure 1.1 – Alongship and Athwartship angles (from Lanzoni [15])

The current MBES calibration methods are able to produce excellent results with regard to 3-D beam patterns when the measurements are conducted in a controlled environment. MBES don't feature split-beam capabilities in both dimensions (alongship and athwartship), so they don't allow for precise point target localization. As a result of this, calibration spheres must be incrementally positioned along the beam in both alongship and athwartship directions [13]. Consequently, these methods are very time consuming, often to the point that the amount of time required exceeds the amount that can be realistically permitted in a schedule [15]. Furthermore, these reference spheres act as a poor representation of the seafloor, which typically behaves as an extended surface target [11]. An extended surface target is a target that extends beyond the beam footprint of a sonar. An extended surface target is believed to be a better representation of the seafloor than a round sphere [10].

As a result of this motivation, a suspended “Jack-Chain” target was constructed and used to calibrate a Reson T20-P MBES. Previous calibrations of MBES’s using a 38.1 mm WC sphere took several weeks of data collection to complete because the calibration spheres had to be incrementally positioned throughout each beam [15]. Calibrations with the jack-chain extended target can be completed in a reduced time period because the target extends beyond the beam footprint and allows for a more efficient calibration “sweep” in which every beam of a MBES is moved across the target. If an extended surface target is acoustically characterized then it permits a user to calibrate a MBES system for intensity measurements in an efficient manner with a target that is similar in morphology to that seen in the field.

In this work, an alternative intensity calibration target was developed and tested with a Reson T20-P MBES in the test tank facilities at the University of New Hampshire. This MBES is a 200 kHz sonar with 256 beams. Once the T20-P MBES was calibrated in the tank, it was used to collect backscatter in the field, along a survey line in Portsmouth Harbor, Portsmouth, NH. A simpler and more easily calibrated 200 kHz split-beam echo-sounder (SBES) was used to both acoustically characterize the new calibration target and to assess the validity of the T20-P MBES measurements in the field.

CHAPTER 2

EXTENDED TARGET DESIGN, CONSTRUCTION, AND ACOUSTIC CHARACTERIZATION

2.1 – Design and Construction

Standard calibration spheres behave as discrete targets with backscatter characteristics that are independent of incident angles, and have known target strength (*TS*) values depending on their size and material [23]. *TS* is a measure of a targets ability to scatter sound. The commonly used standard calibration spheres are small compared to the beam-width of most SBES and MBES, making them useful for determining *TS* but they don't directly provide estimates of surface scattering strength (*Ss*) [15]. *Ss* is the reflectivity characteristic of a unit area, intrinsic to the target [11]. As an alternative, an extended target comprised of many random scattering elements could be used to provide a calibration that directly tests the accuracy with which SBES or MBES systems can estimate *Ss*. The *Ss* variable becomes *Sb* by convention when in reference to actual seabed backscatter strength, which is a quantity that is desirable when characterizing seafloor habitat. Accordingly, a prototype extended target constructed from jack-chain was built and tested at the University of New

Hampshire's Center for Coastal and Ocean Mapping/Joint Hydrographic Center (UNH CCOM/JHC).

One motivation behind the design of this target was the goal of simulating the seafloor in a controlled environment. The goal was to have a target that resembled a simple first order model of the seafloor, where a large number of random scattering 'centers' exist. If the number of random scattering elements is large enough, then the central limit theorem can be applied, and the backscatter should display a Rayleigh distribution [11]. If the jack-chain target is treated as a collection of small scattering elements, then the total expected scattered pressure can be estimated as the sum of the random scattered pressure per element (link) in conjunction with the similarly random phase of the individual return per element [11]:

$$P_{s,tot} = \sum_{k=1}^{N} P_{s,k} e^{j\emptyset_k} \tag{2.1}$$

where $P_{s,tot}$ is the total scattered pressure return, and P_s is the scattered pressure per link. *N* is total number of scattering elements included in the beam footprint, *k* is the scattering element index, and $\emptyset$ describes the phase of the individual return, and *j* is the complex variable. If the scattering elements have comparable amplitude and are not grouped together in tightly bound groups, then the Central Limit Theorem states that both the real and imaginary parts of the complex backscattered pressure (P_s) should obey Gaussian statistics, at least

approximately [11]. Additionally, the complex backscattered pressure is generally assumed to be a Gaussian random process [1] and the envelope will have a Rayleigh probability density function (PDF) [11]. The Rayleigh distributed envelope is a result of the backscatter pressure originating from a large number of independent scattering elements.

The extended target was constructed of stainless steel, type 18, jack-chain. Stainless steel was selected for its durability and its ability to resist corrosion. Jack-chain was selected for its single link symmetry. Approximately 200, two meter long lengths of chain were assembled in the style of a curtain, fixed at the top and bottom by fiberglass supports. The lengths of jack-chain were not fixed rigidly in any way other than to the support frame. This allowed the links to be suspended in a random orientation. Holes were drilled one cm apart from each other to provide consistent spacing between lengths of chain. Lengths of chain were threaded into the top support using fishing line and a needle. The final extended target measured two meters on a side, with spacing between individual scattering elements approximately equal to one cm. An image of the target is included in Figure 2.1.

Figure 2.1 – Jack-chain extended target (entire target left, close up right)

The Acoustic test tank in the Chase Ocean Engineering Laboratory at the University of New Hampshire was utilized to conduct the experiments. This tank measures 18 m long x 12 m wide x 6 m deep (60 feet long x 40 feet wide x 20 feet deep). The tank features a primary powered bridge mounted on a rail system. The powered bridge allows for variable positioning along the 18 m length of the tank. A powered cart is mounted to the powered bridge which allows for further variable positioning along the 12 m width of the tank. A programmable rotating controller is mounted to the powered cart and allows for precise angular positioning of the carbon-fiber transducer mounting pole. This pole is mounted in a chuck and is able to be lowered into the water using a power winch. This pole allows for variable depth positioning in the tank. The

secondary bridge is primarily used for mounting reference hardware and/or hydrophones. The test tank facility is illustrated in Figure 2.2.

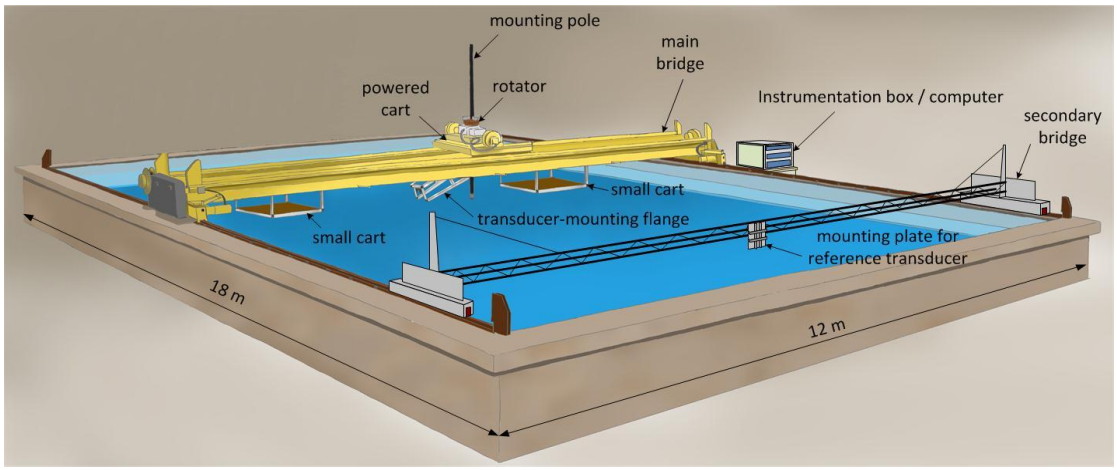

Figure 2.2 – Acoustic test tank at UNH (from Lanzoni [15])

2.2 – Acoustic Characterization of the Extended Target

A 200 kHz SIMRAD EK60 SBES was used to acoustically characterize the extended target during experiments in the test tank. The EK60 SBES was used to characterize the target because it is more easily calibrated than a MBES. The EK60 SBES is more easily calibrated because the split-beam capability allows for precise point target localization and permits a user to monitor target location in real time. This sonar operates in the mode of a piston transducer with a 7°, -3dB beam-width. Figure 2.3 shows the combined transmit and receive beam pattern of the EK60 SBES.

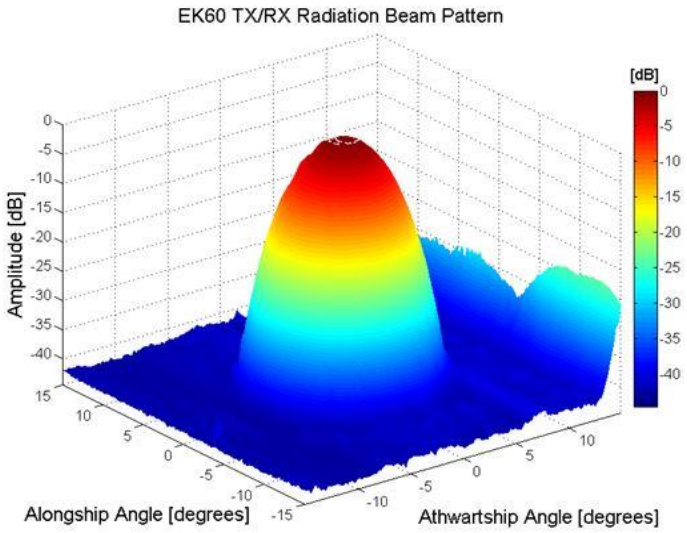

Figure 2.3 – 3-D EK60 SBES transmit/receive beam pattern (from Lanzoni, personal communication)

In the case of this transducer, the main lobe of the beam is conical. The SBES was operated in active mode with a pulse length of 128 µS, and this system was set to ping at a rate of four pings per second. The pulse length and the operational mode stated here were used for all of the efforts with the EK60 SBES presented in this thesis. *TS* measurements of the jack-chain extended target were collected using this SBES during the characterization. These *TS* measurements were used to determine the surface scattering strength, *Ss* of the new target.

TS can be regarded as the relative portion of the pulse intensity that is redirected back to the receiver with a measurement reference range of 1m from the target [17]. This term describes how reflective the target was for a particular measurement configuration. In the case of an extended surface target such as the jack-chain target investigated here, *TS* is defined by equation 2.2 [17].

$$TS = Ss + 10\log(A) \tag{2.2}$$

In this equation, *Ss* is the Scattering Strength (in dB / 1 m²), and *A* is the insonified, or illuminated area (m²). Equation 2.2 shows that *TS* is the response of the insonified target while *Ss* is the reflectivity characteristic, intrinsic to the target [10]. The scattering strength, *Ss* can be directly determined from equation 2.2. Scattering from an extended target is usually quantified by the scattering strength and while this value is able to be calculated from equation 2.2, a more detailed discussion of scattering strength is presented in equation 2.3 and equation 2.4:

$$< |P_s| >^2 = |P_i|^2 A\sigma \frac{1}{r^2} \quad (2.3)$$

$$Ss = 10log_{10}\sigma \quad (2.4)$$

Where $< |P_s| >$ is the ensemble average of the scattered pressure, P_i is the incident pressure, *A* is the insonified area, *r* is the range to the target, σ is the scattering cross section, and Ss is the scattering strength [11]. If a backscatter measurement is recorded several times using the same measurement configuration, but for an ensemble of statistically equivalent target patches, then the scattered mean square pressure fluctuation will be proportional to the squared incident pressure and the area of the patch. The scattered pressure will be inversely proportional to the squared range [11].

An initial effort was conducted with the previously described EK60 SBES to acoustically characterize the extended jack-chain target once it was constructed. Validation was required to confirm that this calibration target truly does behave in a manner consistent with similar extended surface targets, like a featureless segment of seafloor [10]. An investigation into the jack-chain targets backscatter response at various angles of incidence, and at various ranges was conducted. All of the measurements related to these investigations were recorded with the 200 kHz SIMRAD EK60 SBES and the *readEKRaw EK/ES60 ME/MS70* MATLAB toolkit written by Rick Towler (NOAA Alaska Fisheries Science Center) was used to extract the data from the raw files [25]. *TS* measurements of the entire target were recorded as a function of incident angle at a normal range of six meters. The target was suspended in the tank from a

floating platform with the middle of the target at the same depth as the EK60 SBES. This platform was placed at varying positions along the length of the tank corresponding to 5° incremental changes in the angle of incidence. This concept is illustrated Figure 2.4.

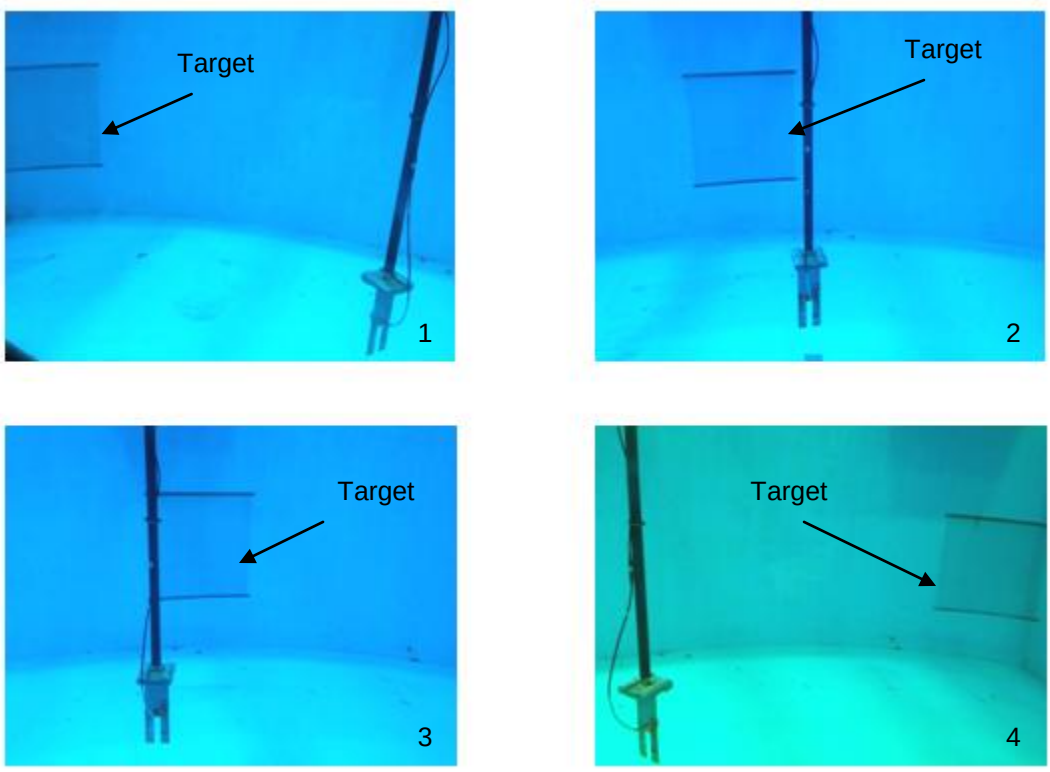

Figure 2.4 – Positioning of target for angular dependence of *Ss* investigation (left to right, top to bottom)

One should look at Figure 2.4 and follow the progression of images labeled one through four in the bottom right of each panel. Each new target orientation was a new measurement. A laser level was used to ensure proper beam alignment to the jack-chain target. The laser level was directed towards a paper target fixed to the floating platform which corresponded to the chain targets position underwater. This alignment method is shown in Figure 2.5.

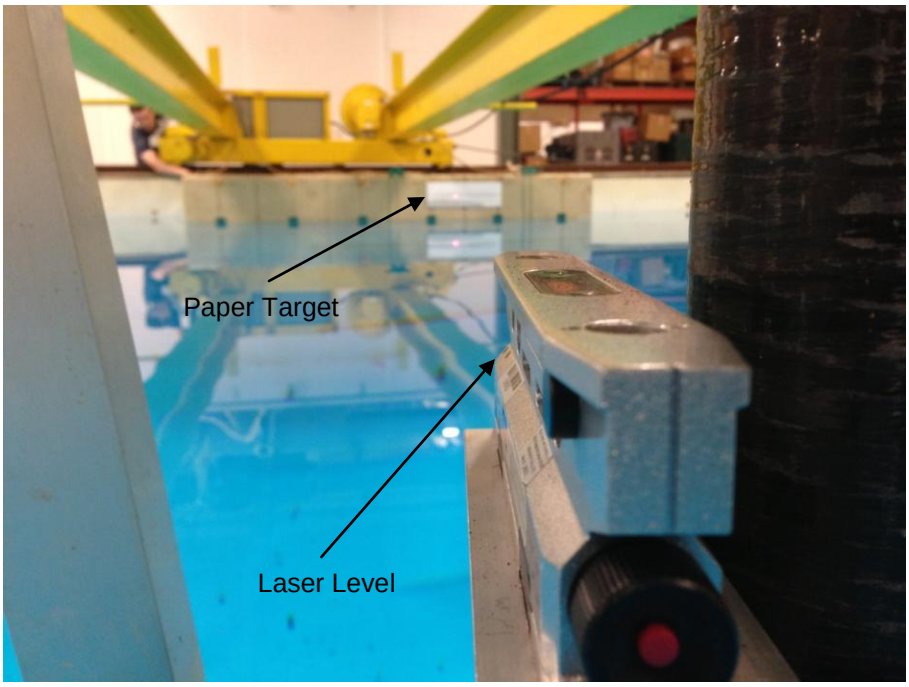

Figure 2.5 – Laser level alignment method with paper target corresponding to calibration target position

In Figure 2.5, the laser level is directed towards a paper target fixed to the floating platform that the extended chain target is suspended from. The laser aims at a point that corresponds to the middle of the underwater extended chain target. This alignment method ensures that the beam is incident on the middle of the target, as shown by Figure 2.6. Figure 2.6 is a drawing to show this alignment method at six meters.

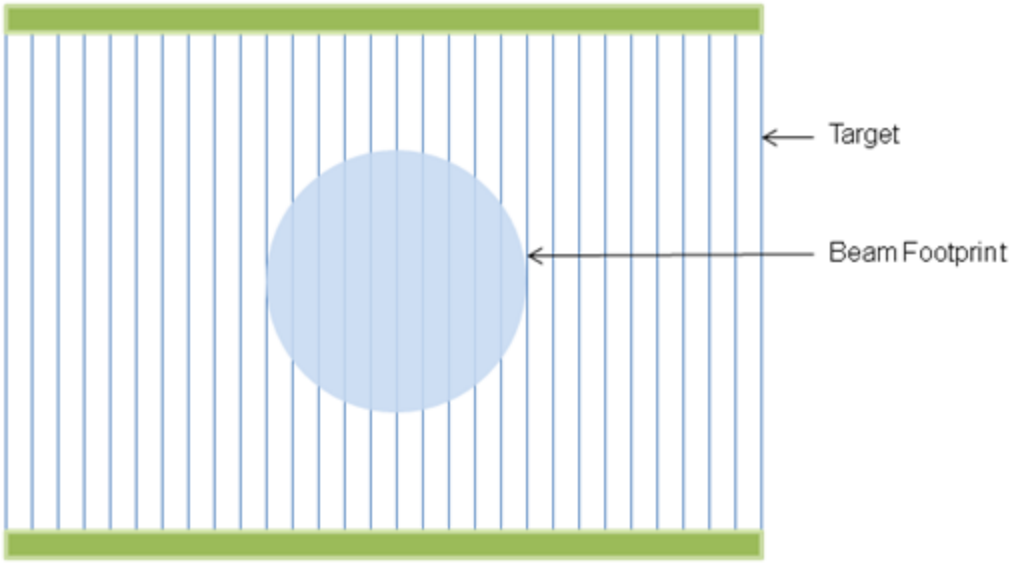

Figure 2.6 – Beam interaction with target

TS values from this experiment show angle dependence with higher *TS* values near normal incidence and lower *TS* values at oblique incidence (Figure 2.7, left), approximately tracking the beam footprint size as it changes with incidence angle. An average value of all the trials at each angle is included in Figure 2.7.

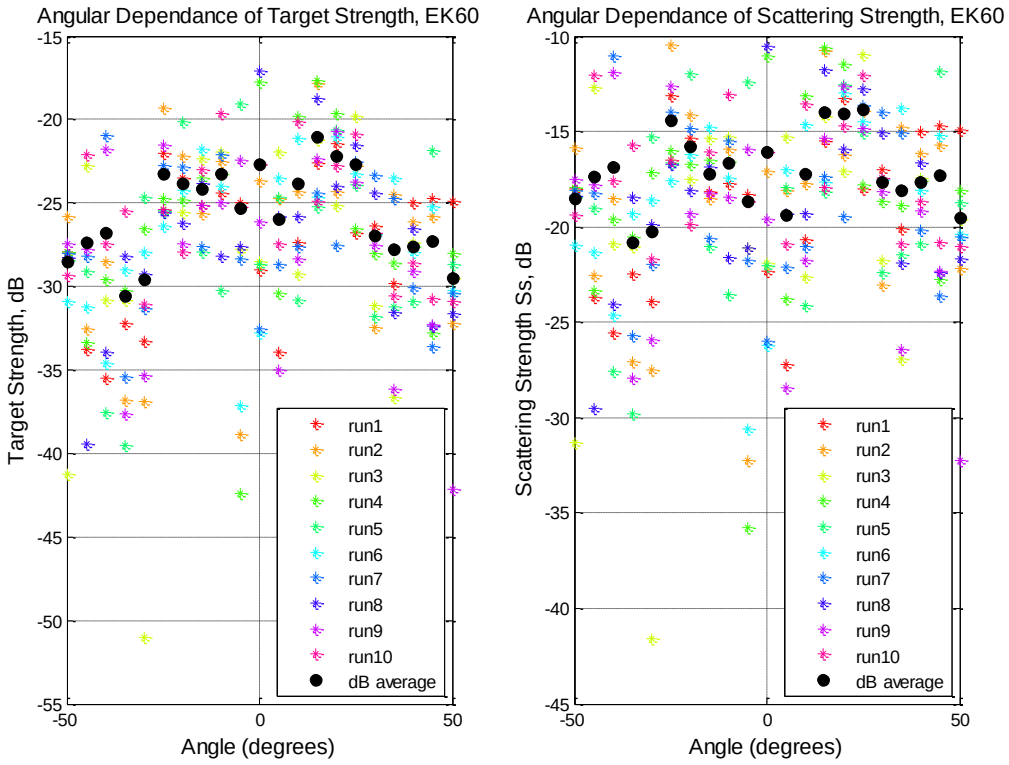

Figure 2.7 – *TS* (left) and *Ss* (right) as a function of incident angle

Ten sets of measurements, or runs, spanning the length of the test tank were recorded, and are outlined in the legend of Figure 2.7. Average *Ss* values show weak or no angle-dependence. This is the expected type of distribution from a uniformly random target made of many independent scattering elements where the Central Limit Theorem applies, as described by Urick [26]. The *Ss* data was condensed independently of angle and was used to estimate the PDF of the equivalent amplitude. The PDF is compared to a Rayleigh distribution in Figure 2.8. The Rayleigh parameter was found to be equal to 0.1025 and was determined from the maximum likelihood estimates of the empirical Rayleigh distribution fit to the data.

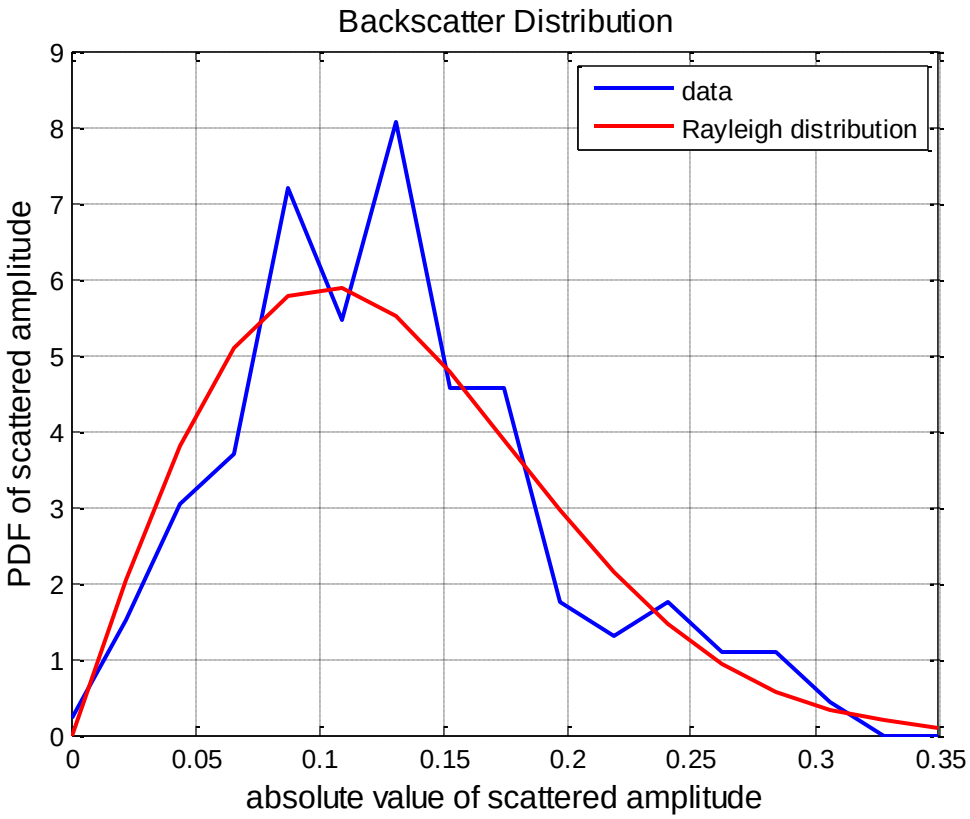

Figure 2.8 – Comparison of the scattered amplitude distribution (blue histogram) with a Rayleigh distribution (red curve)

A Rayleigh distribution is the typical distribution expected of backscatter over a flat, featureless seabed [11], and qualitative agreement between the data and a comparison Rayleigh distribution is displayed in Figure 2.8. To further evaluate this backscatter data, a Kolmogorov-Smirnov statistical test (KS-test) was employed to confirm the hypothesis of Rayleigh distributed backscatter from the extended chain target. The KS-test is a non-parametric measure that describes how well a theoretical CDF (Cumulative Distribution Function) fits the CDF estimated from observed data [1, 20]. The P value describes how likely it is that the observed data was drawn from the distribution in question, and can be

determined from the KS-test. If the P value is below 0.05 it would be very unlikely for the data to be drawn from a Rayleigh distribution. If the P value is above 0.05, and particularly if it's well above 0.05, then it is likely that the data was drawn from a Rayleigh distribution. P was equal to 0.2146 for the SBES data from the extended chain target, suggesting that the data does fit a Rayleigh distribution.

The range dependence of the *TS* and the *Ss* was investigated. This was done in order to simulate a narrower beam system, like a 2° x 2° MBES. As the SBES approaches the chain target, fewer chain links contribute to the backscatter. This could pose a potential problem with regard to the Central Limit Theorem. The Central Limit Theorem is significant for the simple seafloor models presented here, and applies when there are a large number of independent scattering elements. The Central Limit Theorem may not apply during measurements that limit the number of contributing scattering elements. These measurement configurations are similar to what a narrow beam MBES would experience from a larger range measurement. The jack-chain target was again suspended from a floating platform and was held stationary at normal incidence to the EK60 SBES. The powered cart on the bridge of the test tank was used to vary the range between the SBES and the target. As the range between the SBES and the target changed, the insonified area would change as well, thus including different numbers of scattering elements (links). For example, at two meters approximately 240 links are included in the 7° SBES

footprint and at seven meters there are more than 2900 links included. A 2° x 2° MBES would include roughly 780 links at 8 meters.

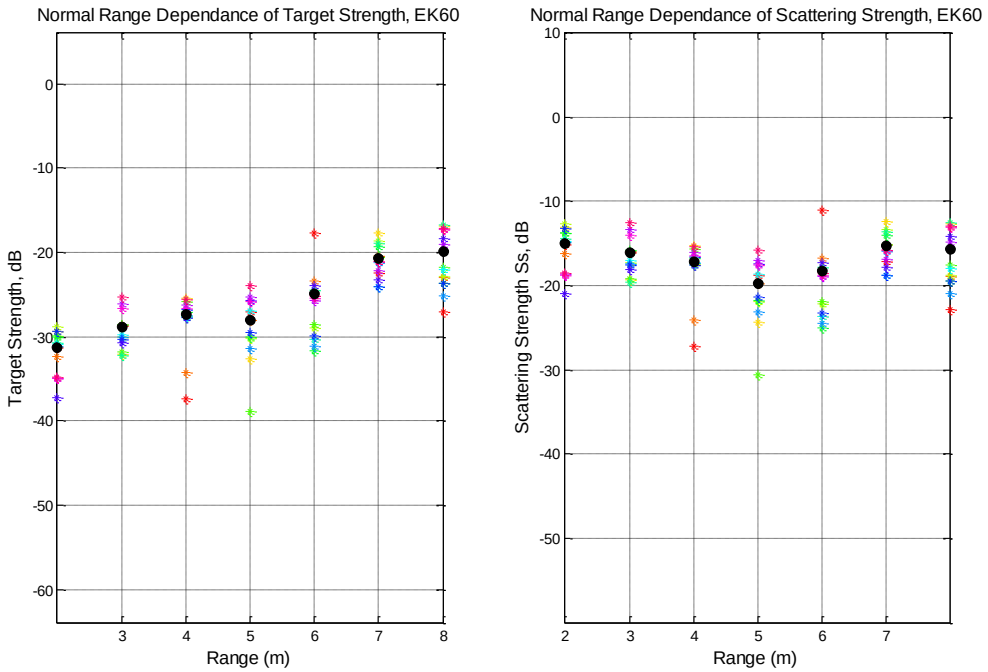

Figure 2.9 – *TS* and *Ss* as a function of range at normal incidence

Figure 2.9 shows that the *TS* values increase with range, which is expected due to the dependence of *TS* on the insonified area. More scattering elements are included as the beam footprint grows with range from the target. A higher signal is returned with more contributing scattering elements, and a higher *TS* value is measured. The *Ss* obtained after compensation of the insonified area shows a behavior that is independent of the measurement range, confirming that the measurement configuration is correctly compensated. The trend displayed in Figure 2.9 shows that the *TS* depends on the number of active scattering elements, but the *Ss,* intrinsic to the target, does not show this

dependence. These SBES range measurements show how the number of scattering elements included in a measurement has a direct impact on the measurement value, and that the SBES footprint approximates the footprint of a narrow beam MBES at close range. Furthermore, these results support the claim that this target truly does behave in a manner consistent with simple seafloor models, where the total return pressure is composed of individual contributing returns from many independent scattering elements.

2.3 – Discussion

The results from the jack-chain target showed little dependence between the angles of incidence and the *Ss* values, suggesting that the target *Ss* is independent of the angle of incidence. This was expected for the extended chain target because the chain links are suspended in a random orientation. The backscatter from the target was also found to be Rayleigh distributed from statistical testing.

The *TS* values increase with range, which is expected due to the dependence of *TS* on the beam footprint. The *Ss* obtained after compensation of the insonified area shows a behavior that is independent of the measurement range, confirming that the measurement configuration is correctly compensated. This makes the target advantageous in MBES calibration because the *Ss* value of the target will be the same for every beam of a MBES. The final *Ss* value that is representative of the jack-chain extended target was found to be equal to -16 dB based on the measurements presented in this chapter.

The efforts summarized here are to support the claim that this target is suitable for MBES calibration. The tests were conducted to show that the *Ss* values are independent of measurement geometry and that the *TS* depends on the number of active scattering elements. These are all desirable features for

calibrating MBES, and the target is justified for use in MBES calibration based on these claims.

CHAPTER 3

MULTI-BEAM ECHO-SOUNDER CALIBRATION

3.1 – Introduction

In MBES operation, hundreds of beams are formed over a wide angular sector in the athwartship direction by taking the coherent sum of time delayed return signals originating within the elements of a transmit array and received by the elements of a co-located receiver array [17]. Seafloor backscatter can be extracted from each individual beam through the amplitude of the portion of the complex envelope associated with the seafloor [11].

MBES calibrations can include many parameters like gain and source level offsets [13]. These are manufacturer applied quantities that can be calibrated as separate terms. Additional factors must be considered in order to convert the digital value that is reported from a Reson record into a meaningful echo-level present at the transducer face [15]. These factors include transduction, which is the actual conversion of an acoustic pressure wave into an analog voltage. The process of digitization or converting this analog voltage to a digital number must be considered as well. Time delay beam-forming is another factor that requires

analysis. These effects are difficult to separate individually, but are able to be summarized with a “catch-all” calibration coefficient [15]. The calibration coefficient accounts for many of these topics and is a subject of interest. The final output of this work is an angle, and thus beam-dependent calibration coefficient, *C*, which is calculated from the sonar equation. Approved calibration results could be applied to backscatter data sets collected with the MBES system and this would produce calibrated acoustic backscatter.

The MBES system that was calibrated in the UNH tank was a NOAA owned 200 kHz Reson T20-P MBES (Projector: TC2181, S/N 2413031; Receiver: S/N 2313068). At 200 kHz the manufacturer states that this system features a 2° transmit beam-width, and a 2° receive beam-width at broadside. In the configuration that was used for this effort, 256 beams were spread over a 140° degree swath with a 130μS pulse-length. The MBES transmitter and receiver are mounted orthogonally to each other. Figure 3.1 shows the mounting arrangement.

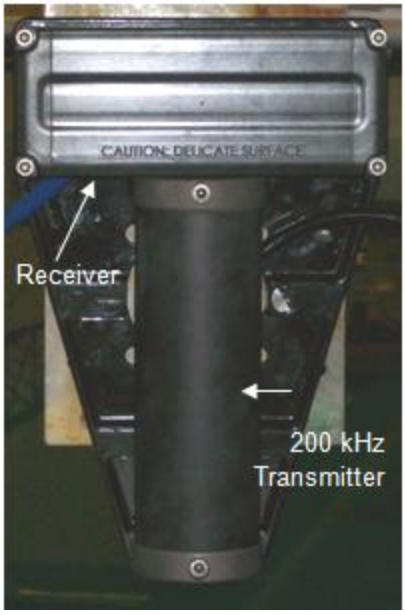

Figure 3.1 – T20-P MBES mounting configuration (receiver top, 200 kHz transmitter bottom)

A separate array is used for both the transmitter and the receiver. This configuration is known as a Mills-Cross [17]. In a Mills-Cross configuration, one transducer transmits while the other transducer is mounted orthogonally to the first and acts as the receiver. The resulting beam pattern is the product of the beam pattern for each transducer. The combined transmit/receive beam pattern for this arrangement produces a narrow, pencil-like beam as shown in Figure 3.2.

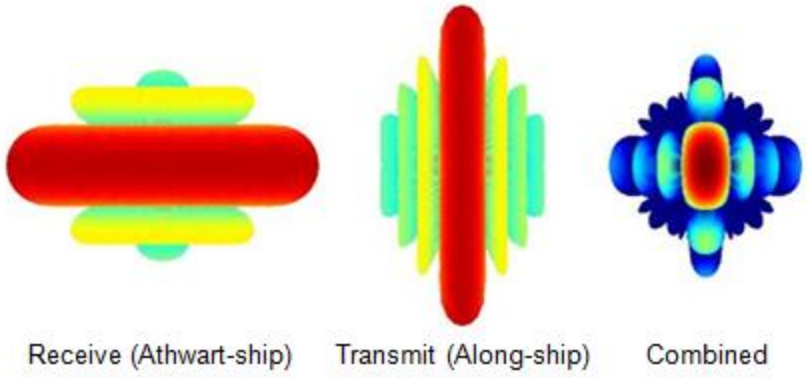

Figure 3.2 – Mills-Cross example beam pattern (single beam, receive left, transmit middle, combined right, from Lanzoni [15])

Figure 3.2 shows the region of maximum intensity on-axis for both transmission and reception. The red areas show the maximum, and side lobes are present in each picture. This type of directivity has the advantage of producing high angular resolution in both the alongship and athwartship directions [26].

3.2 – Calibration Coefficient Development

As an acoustic pulse is emitted from the transducer, it propagates through the water column, interacting with the medium along its route until it reaches a target. Upon the pulse's arrival at a target, the sound scatters and a portion of this scattered sound, the backscatter, returns to the transducer. The sonar equation describes this process in a quantifiable manner, using values presented in units of decibels (dB), a logarithmic representation of acoustic intensity. The basic active sonar equation is given by equation 3.1:

$$EL = SL - 2TL + TS \tag{3.1}$$

where *EL* is the echo-level at the transducer face in dB (re: 1µPa), *SL* is the source level in dB (re: 1µPa), *TL* is the transmission loss in dB/m (re: $1m^2$), and *TS* is the target strength in dB (re: $1m^2$), from a reference distance of 1 meter away from the target [26].

The transmission loss term accounts for the energy lost due to the spreading and absorption of the acoustic pulse. Equation 3.1 describes the process for an active acoustic transducer, where the pulse is emitted and received from the same transducer or transducers that are co-located, thus the transmission loss is applied twice to account for the two-way travel. Transmission loss is a function of range and absorption, as shown in equation 3.2:

$$TL = 20\log(R) + \alpha R \tag{3.2}$$

where *R* is the range from the transducer to the target, and α is the absorption (dB/m).

The target strength is the response of the insonified target and describes how well the target reflects the incident pulse. This term can be broken into its constituent components when considering an extended surface target as previously discussed. In such a case, *TS* can be defined by equation 3.3.

$$TS = 10\log(A) + S_s \tag{3.3}$$

In this equation, *A* is the insonified area, and *Ss* is the surface scattering strength. The beam footprint near normal incidence is constrained by the beam-width. The beam-width limited area term for the MBES is displayed in equation 3.4 [19],

$$A_{bwl} = (\theta_T \theta_R R^2)/\cos(\varphi) \tag{3.4}$$

where θ_T is the transmit beam-width, θ_R is the receive beam-width, φ is the beam steering angle, and *R* is the range. The equivalent beam-width was calculated for both transmission and reception. The equivalent beam-width accounts for side lobe interaction and models an ideal beam of unity response within the beam, and zero response outside the beam [17, 23, 26]. Substituting the sonar equation terms yields the following relation, shown in equation 3.5.

$$EL = SL - 2(20\log(R) + \alpha R) + 10\log(A) + S_s \tag{3.5}$$

The reported *EL* from a MBES system has some user applied gains which must be considered. This additional gain term, *G*, is included in equation 3.6.

$$EL + G = SL - 2(20\log(R) + \alpha R) + 10\log(A) + S_s + G \quad (3.6)$$

A Reson record does not directly measure an echo-level with a user applied gain. Reson records report some digital value (hereby referred to as *DV*) representing the return signal [15]. This *DV* has units uniquely inherent to the system and is often left in "Reson units". The *DV* includes the measured return, the user applied gain and any offsets that were previously unaccounted. These quantities are managed by the "catch all" calibration coefficient, *C*. This concept is summarized by equation 3.7 and 3.8.

$$DV = EL + G + C \quad (3.7)$$

$$DV = SL - 2(20\log(R) + \alpha R) + 10\log(A) + S_s + G + C \quad (3.8)$$

It is now possible to rearrange this equation and solve for *C,* which is shown in equation 3.9:

$$C = DV - SL + 2(20\log(R) + \alpha R) - S_s - 10\log(A) - G \quad (3.9)$$

Once known, the calibration coefficient can be used to convert the *DV* into quantities of interest like *Ss*. The final implementation of this calibration coefficient is presented in its application to calculate calibrated backscatter. This is presented in equation 3.10.

$$S_s = DV - SL + 2(20\log(R) + \alpha R) - C - 10\log(A) - G \quad (3.10)$$

The *Ss* values calculated from equation 3.9 incorporate the calibration coefficient values. These *Ss* values represent the quantifiable backscatter measurement, and can be regarded as calibrated backscatter when the calibration coefficients, *C*, are applied

3.3 – MBES Calibration

Suitable operating parameters for *G* and *SL* must be determined to avoid saturating the system prior to conducting the calibration experiment. Saturation occurs if the system is operated outside of a linear response regime [7]. The reported *DV* is a 16 bit digital number and the dynamic range of a MBES system is bounded by this limitation. If a return signal is actually more intense than what the dynamic range of the MBES system can accommodate, then the MBES clips the signal. This means that the reported *DV* is less than what the physical return signal was, and the measurement is ultimately incorrect. Due to this effect, care must be taken in selecting operating parameters so that saturation may be avoided. This is done by collecting measurements with various combinations of *G* and *SL,* and then reviewing the data to determine suitable settings. These measurements were recorded by manually stepping through power and gain settings in 5 dB increments to determine a suitable linear region within the working dynamic range of the system. The results of these measurements are summarized in Figure 3.3.

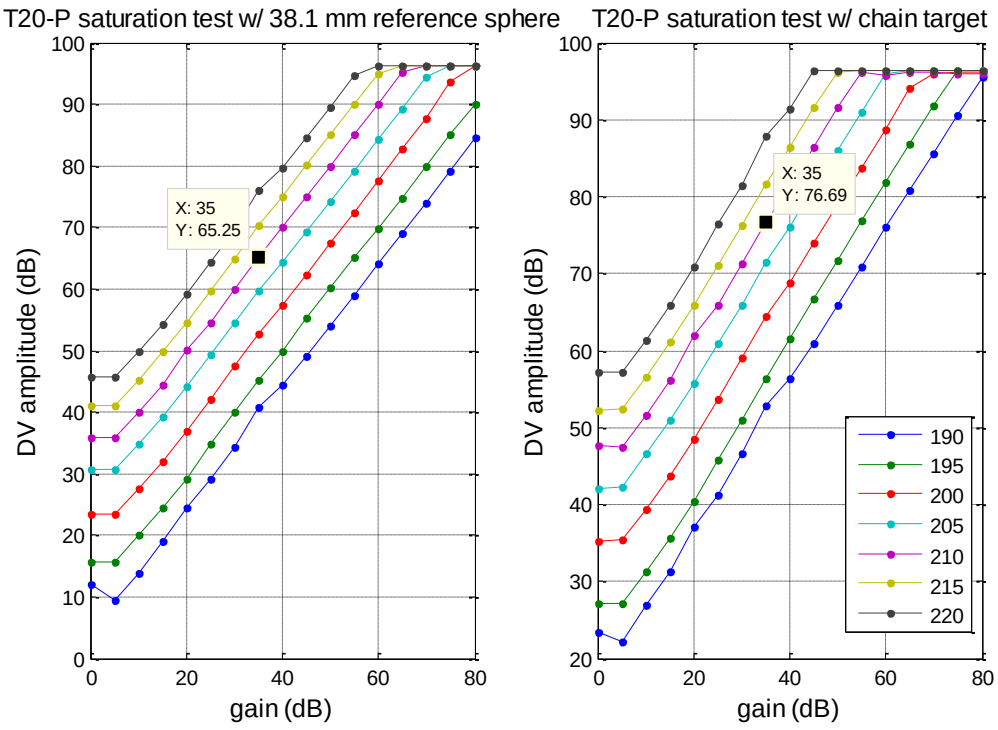

Figure 3.3 – T20-P saturation measurements, gain vs. *DV* amplitude (dB) for several *SL* settings

The colors of each curve represent different *SL* settings, in dB. A hard clip in the return signal is very obvious at the expected saturation point (96 dB). Operating parameters were chosen based on these results, and were selected in a region where the response is linear. Saturation was tested for both the extended jack-chain target and the reference sphere since measurements would be recorded from each target. These operational settings are defined in table 1.

Table 1 – T20-P operational settings summary

Target	Source Level (SL)	Gain Select (G)
Jack-chain extended target and 38.1mm WC sphere	210 dB	35 dB

The calibration experiment was designed to calibrate every beam of the system and this was achieved by rotating the array in 1° increments with the rotator in the test tank facility through 160°, so that all beams were incident on the chain target. The target was suspended from a floating platform which was flush to the back wall of the test tank (as illustrated by Figure 3.4), positioning the target approximately 7.3 meters away from the MBES. The MBES was operated in “best coverage” or equidistant mode, with a 130 μS long, CW (continuous wave) pulse. Equidistant mode maintains the distance between beams incident on a flat target, whereas equiangular mode maintains the angular gap between beams. The sound speed in the tank was measured next to the MBES active face with an Odom Digibar Pro sound speed probe, and was then manually input to the Reson user interface. Absorption in the test tank was equal to 0.01 dB/m, which was determined from the Francois and Garrison 1982 model [6]. This was assumed to be negligible at the short ranges permitted for use in the test tank, and absorption was set to zero in the Reson user interface. The calibration sweep is summarized by Figure 3.4. The sonar was set to ping 30 times per position, and was triggered by a LabView controller at each new position. The 30 ping setting was selected for statistical robustness, and data were recorded for every ping.

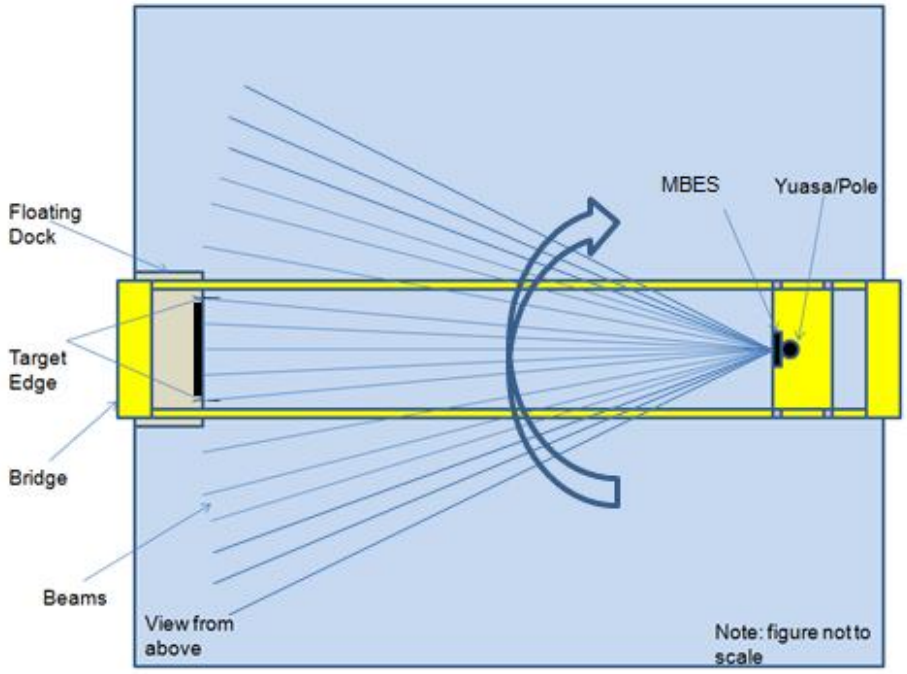

Figure 3.4 – MBES calibration sweep concept

Figure 3.4 outlines the general experiment procedure. As the MBES was rotated, it pinged at the target. The target was manually moved back and forth in a gentle, but random manner (approximately 10 cm in each direction, with a 1 second period) in an effort to ensure an adequate number of independent realizations. The MBES was rotated until the last beam of the swath had moved across the target. This method allows a "sweep" across the target to be completed in a relatively short amount of time and included many independent measurements. Independent realizations are desirable when taking measurements of a uniformly random surface such as the jack-chain target [11]. Recall that the jack-chain target is meant to simulate the seafloor and should

display similar statistics. Independent realizations of the target are required to truly simulate backscatter from a featureless segment of seafloor.

A library of Reson raw data record readers was used to unpack the data, and an echogram (single ping) is shown in Figure 3.5.

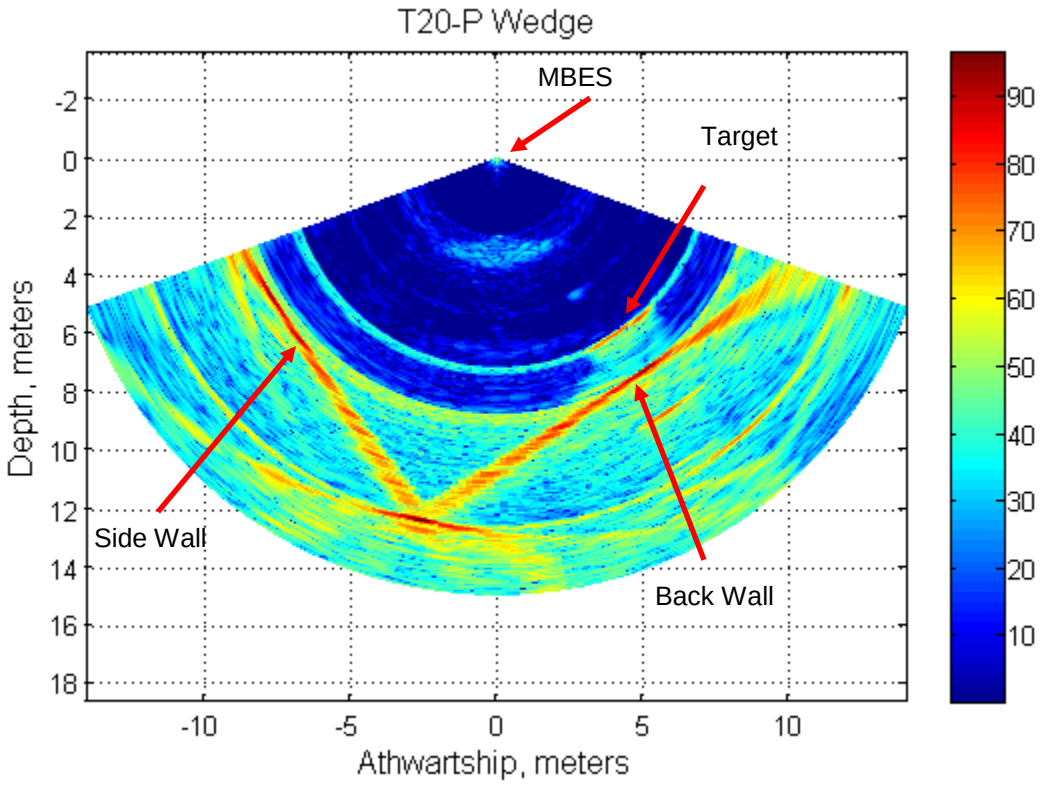

Figure 3.5 – MBES echogram (single ping, midway through calibration sweep)

The color bar in Figure 3.5 describes the received *DV,* in dB. The ping corresponding to the echogram of Figure 3.5 was midway through a calibration sweep across the target. The target is labeled, and can be found at the approximate coordinates (5, 6) on the Figure. The back wall of the test tank is directly behind and parallel to the target. The side wall of the test tank is

orthogonal to the back wall. The distance to the target was known, thus allowing for precise data acquisition around a specific sample window. The *DV* data was then extracted and the calibration coefficient, *C* was calculated per beam.

A threshold detection was implemented to determine all of the pings at which a beam was on the target. Once all the pings that returned a *DV* over the threshold for a given beam were known, then the median ping from this list was determined. This median ping was considered to be the ping at which the beam in question was on the middle of the target. These steps were taken in an effort to mitigate the risk of including detections that were not fully on target. Once the middle ping was known, an additional 150 pings were taken on either side of it. This produces a population of 300 pings per beam spread across the width of the target, thus ensuring an adequate number of independent realizations. The boundaries outlining the data that was used are shown in the following figure as black lines. The purple box is an example to show how the data were averaged (300 pings for each beam) bounded by the black line. This is displayed in Figure 3.6.

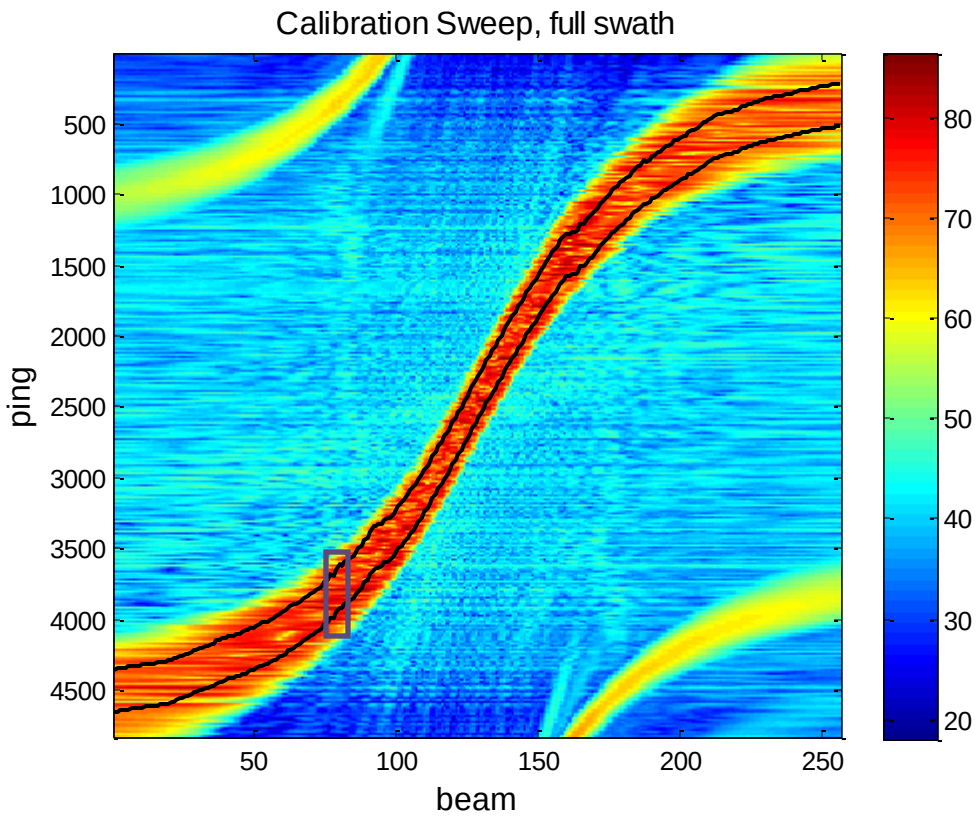

Figure 3.6 – Ping progression with data boundaries of 300 pings (black lines)

The color bar in Figure 3.6 describes the received *DV,* in dB. The 300 ping data slice that was used for beam 82 is included as an example in Figure 3.7 to illustrate the independence of each realization.

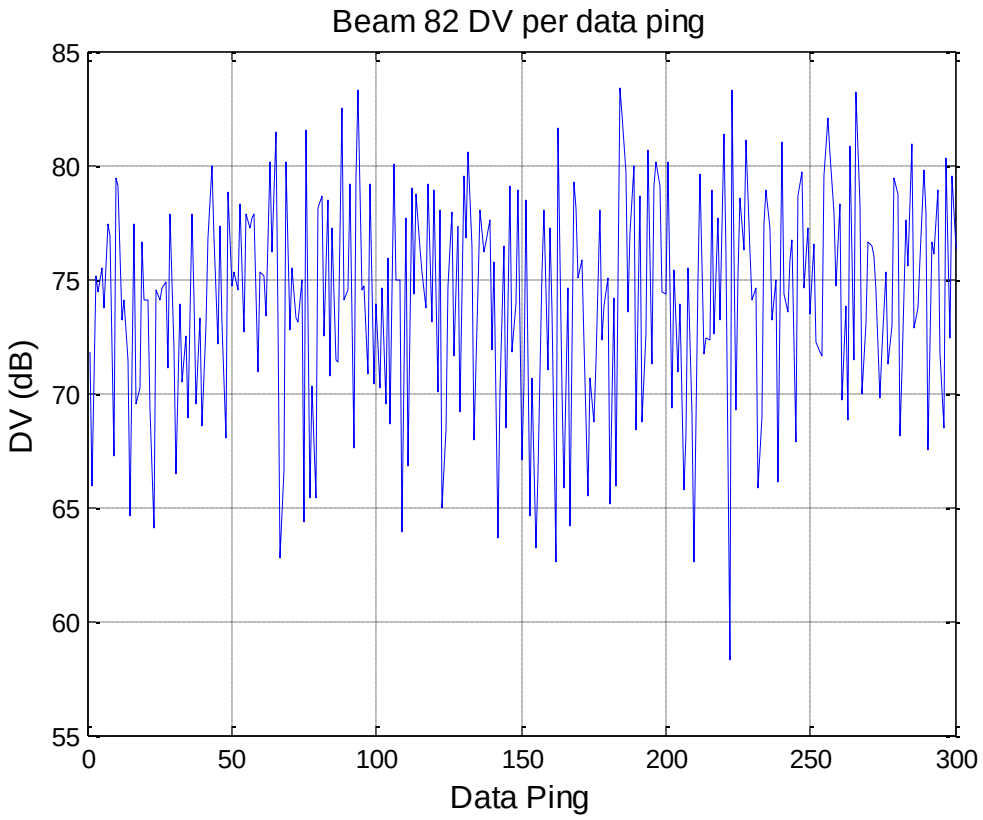

3.7 – Independent realizations of beam 82

A Kolmogorov-Smirnov statistical test (KS-test) was used again to investigate the Rayleigh distributed nature of the 300 ping dataset per beam. The KS-test was performed on the data from every beam. The results of this test for beam 82 are included here as an example. For beam 82, P = 0.7106. Based on these findings it is likely that the data from beam 82 was drawn from a Rayleigh distribution. A plot of beam steering vs. P value is included in Figure 3.8.

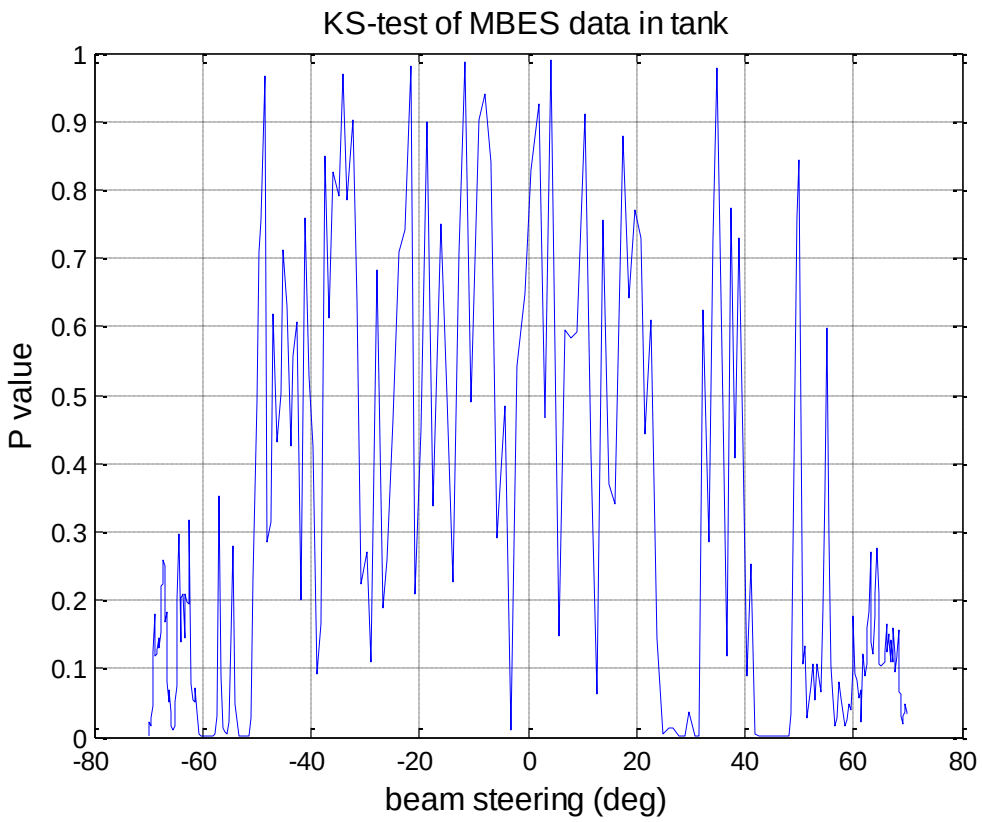

Figure 3.8 – P value from the KS-test calculated for every beam

The majority of the beams display a P value greater than 0.05 (183 out of 256 beams), suggesting that Rayleigh distributed backscatter was achieved. The 300 ping population per beam was used to represent an average *DV* of each beam when it was on the target. Once an average *DV* per beam was determined, the sonar equation was used to calculate the calibration coefficient, *C*. To serve as a calibration comparison unique to the system, select measurements with a 38.1mm WC calibration sphere were recorded for clusters of beams steered to -45°, 0°, and 45°. Measurements were recorded while incrementally lowering the sphere through the beam in the alongship direction and incrementally sweeping across the sphere in the athwartship direction.

These increments provided confidence that measurements were recorded while the sphere was located on the maximum response axis (MRA) of each beam in a cluster. Recall that a typical sphere calibration would require a prohibitive amount of time to complete, so select clusters of beams act as a valid calibration check and comparison unique to one system that is still relatively time efficient. The sonar equation was utilized again, but corrected to accommodate a discrete point target instead of an extended surface target. Thus, the area and *Ss* terms are replaced with a known *TS* value, as shown in equation 3.11.

$$C = DV - SL + 2(20\log(R) + \alpha R) - TS - G \tag{3.11}$$

The ComputeSolidElasticSphere matlab tool [3] was used to model the 38.1 mm WC calibration sphere that was employed for these measurements. This matlab tool requires several inputs from the user to accurately calculate the *TS* of a calibration sphere. The material of the sphere, sound speed, frequency, and bandwidth are some of the primary inputs. The *TS* of the sphere from this model was found to be equal to -39.2 dB. This value was used in the sonar equation calculation of *C* to serve as a comparison to the chain target calibration. Figure 3.9 shows the *C* value comparisons between both the chain and the spheres.

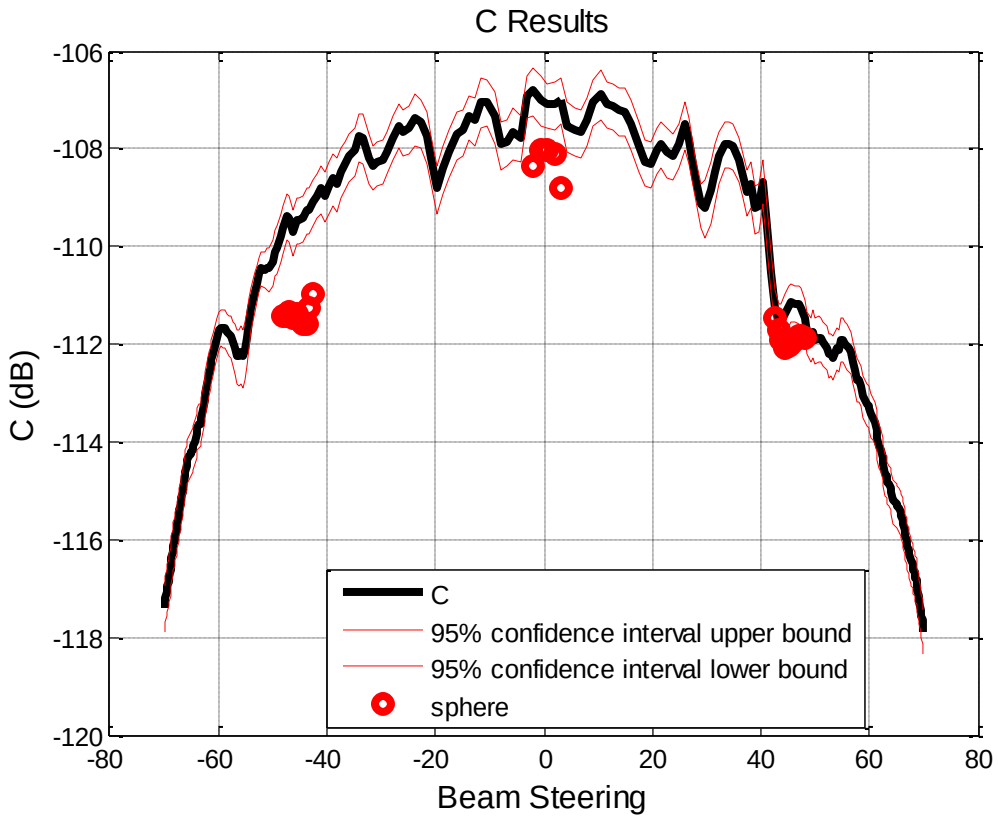

Figure 3.9 – Calibration curve with 38.1 mm WC sphere comparisons at -45°, 0°, and 45°

A meaningful procedure for estimating parameters of random variables uses the calculation of an interval that includes the estimated parameter and a known degree of uncertainty [1]. To that end, error was calculated at the 95% confidence interval and is plotted in red both above and below the calibration curve results. The upper and lower error bounds were calculated from equations 3.12 and 3.13 respectively,

$$C_{upper} = 10log_{10}(DV + \left(\frac{1.96 * \sigma}{\sqrt{n}}\right)) - SL + 2TL - Ss - 10log_{10}(A) - G \quad (3.12)$$

$$C_{lower} = 10log_{10}(DV - \left(\frac{1.96 * \sigma}{\sqrt{n}}\right)) - SL + 2TL - Ss - 10log_{10}(A) - G \quad (3.13)$$

where σ is the standard deviation and n is the number of independent pings.

One can see from Figure 3.8 that the sphere C values are close to the 95% error bound of the calibration sweep C values. Based on these results, the final steps of this work involve field trials of the T20-P MBES with application of the tank calibration to the field data.

CHAPTER 4

MULTI-BEAM ECHOSOUNDER FIELD TRIALS

4.1 – Field Work with T20-P MBES and EK60 SBES

As a test of the tank calibration methodology, the T20-P MBES was used to conduct a field survey. This field work effort was part of the greater NEWBEX (NEWcastle Backscatter EXperiment) project at the Center for Coastal and Ocean Mapping/Joint Hydrographic Center (CCOM/JHC). The purpose of the NEWBEX project is to classify and characterize a segment of seafloor local to the New Hampshire seacoast area. Upon its completion, this characterized segment of seafloor will serve as a 'standard line' that can be run on hydrographic surveys as a means of confirming proper system performance and monitoring system health in the field. This standard line is displayed in Figure 4.1 as the thick black line.

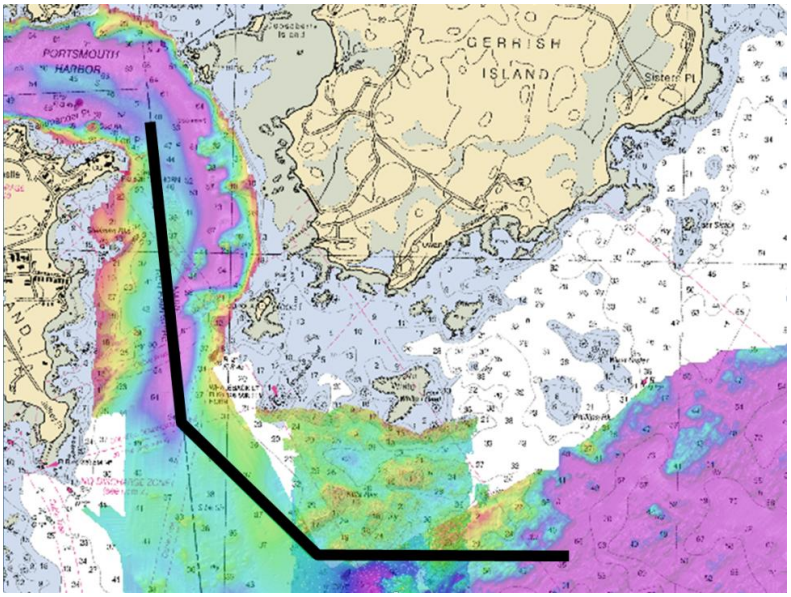

Figure 4.1 – NEWBEX standard line route, Portsmouth Harbor, Portsmouth, NH

The R/V Coastal Surveyor (RVCS), a CCOM/JHC owned and operated coastal research vessel was used to conduct the field work with the T20-P MBES. The T20-P MBES and the EK60 SBES were mounted to the ram of the RVCS, with the EK60 positioned at a 45° angle, as shown in Figure 4.2.

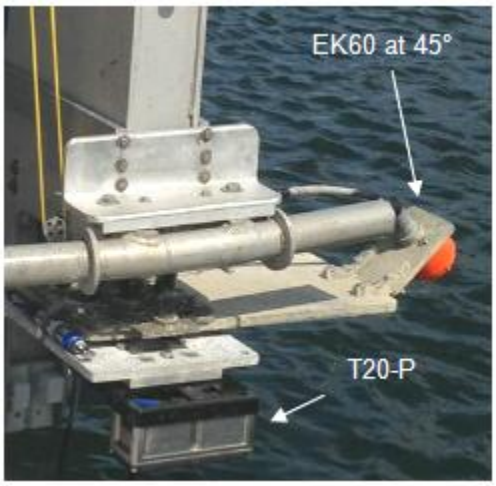

Figure 4.2 – Sonar mounting configuration for field deployment

The EK60 SBES was positioned at 45° because this is a stable region of angle dependant backscatter for most bottom types. This stability presents itself in models at 200 kHz that describe the seafloor backscatter strength in relation to angles of incidence [11]. These models were developed by researchers at the Applied Physics Laboratory (APL) [11] from the University of Washington. The angle dependent backscatter models are outlined in Figure 4.3. One can see that the backscatter values do not change dramatically between 30° and 60°.

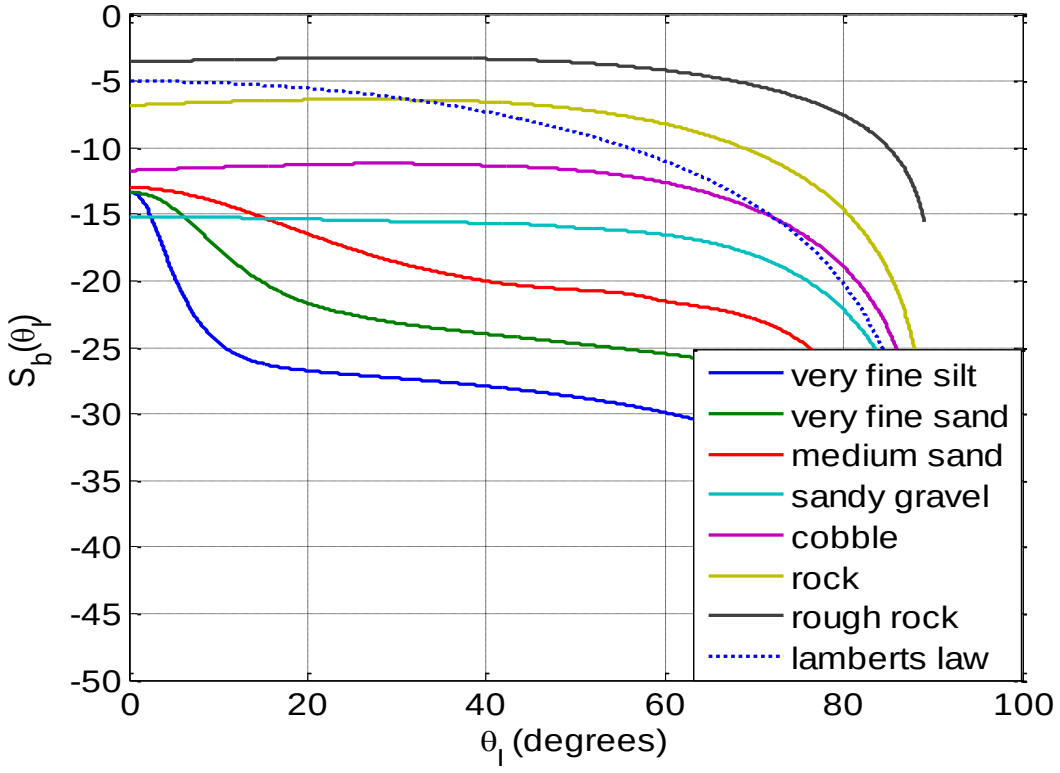

Figure 4.3 – Angle dependant backscatter model, 200 kHz

Sb is seabed backscatter strength, shown on the y-axis. This is the same quantity as surface scattering strength, *Ss*, but in reference to actual seabed measurements.

A trigger controller was employed between the two systems to alternate pings between the EK60 SBES and the T20-P MBES. Each system was set to ping twice per second but the trigger controller alternated between the systems, producing a total of four soundings on the seafloor per second. The line was run out to sea and then back to port, recording data continuously. The same operational settings that were used in the tank for both systems were used again in the field.

The measured *DV* of every ping across the swath for the T20-P is shown in the image scaled plot below, Figure 4.4.

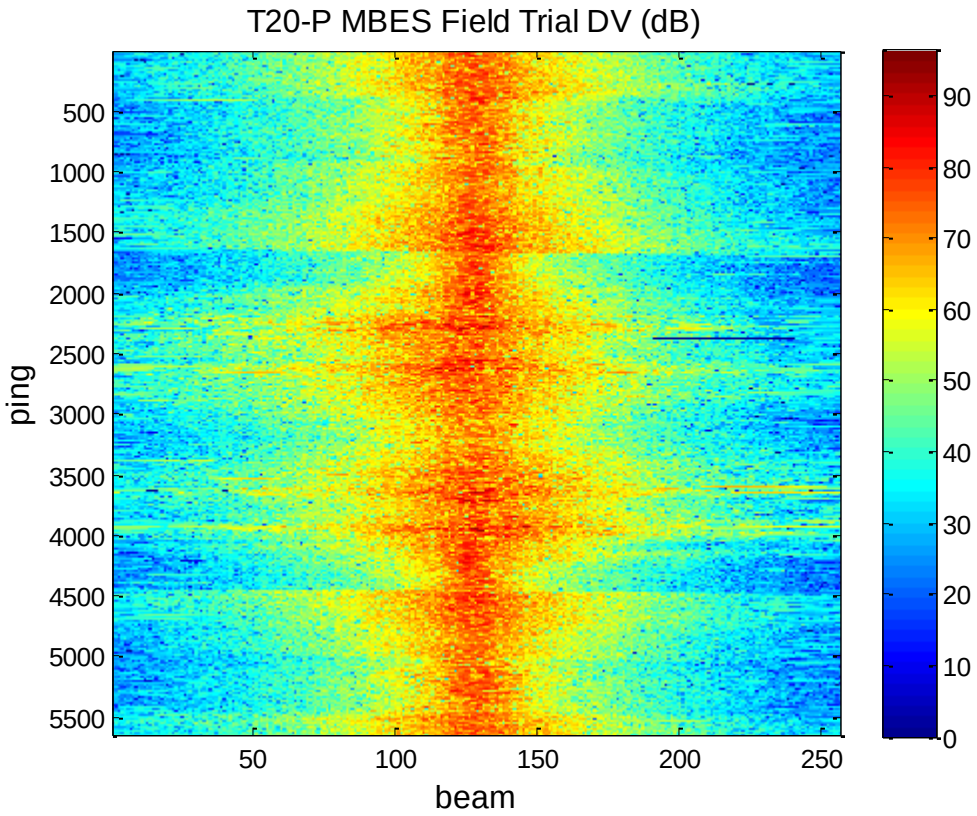

Figure 4.4 – T20-P field trial *DV* (dB)

The quality of these data was then examined by looking for saturation. Saturation occurs for returns over 96 dB but this data set displayed very few returns over this value. There were a total of six detections over this limit, and they were all on the inner, middle beams of the swath (beams 125 to 132), where returns are expected to be the most intense.

Sb was calculated for both systems using equation 3.10 for each ping, taking care to apply the correct calibration coefficient from the tank calibration to the proper beam of the T20-P MBES. Absorption was calculated from the Francois and Garrison, 1982 model [6] and incorporated into the *TL* term. Care was taken on the area calculation in the field. Near normal incidence, the previously listed beam-width limited area equation was used (equation 3.4). This was the case for the calibration work in the test tank. However, near oblique incidence, the beam footprint is typically governed by the pulse length, and equation 4.2 was used:

$$A_{pll} = (c\tau\theta_T R)/(2\,sin\,\theta) \tag{4.1}$$

where c is the sound speed, τ is the pulse length, θ_T is the transmit beam-width, R is the range, and θ is the incident angle to the seabed. Equation 4.1 was used to determine the beam footprint for the *Sb* comparison in the field, since the MRA of the EK60 SBES was directed to an incident angle of 45° and this mounting configuration likely produces a beam that is obliquely incident to the seafloor. A conservative approach however to ensure that the correct area was used included calculating the area for both normal and oblique incidence, but using the

smaller final value. It is important to note that the data from the T20-P beam that was steered to 45° (beam 82) was used because that was the beam parallel to the MRA of the EK60 SBES. This allowed for a meaningful comparison between systems since the data from both sonar's came from the same patch of seafloor. The *Sb* comparison between the two systems is displayed in Figure 4.5.

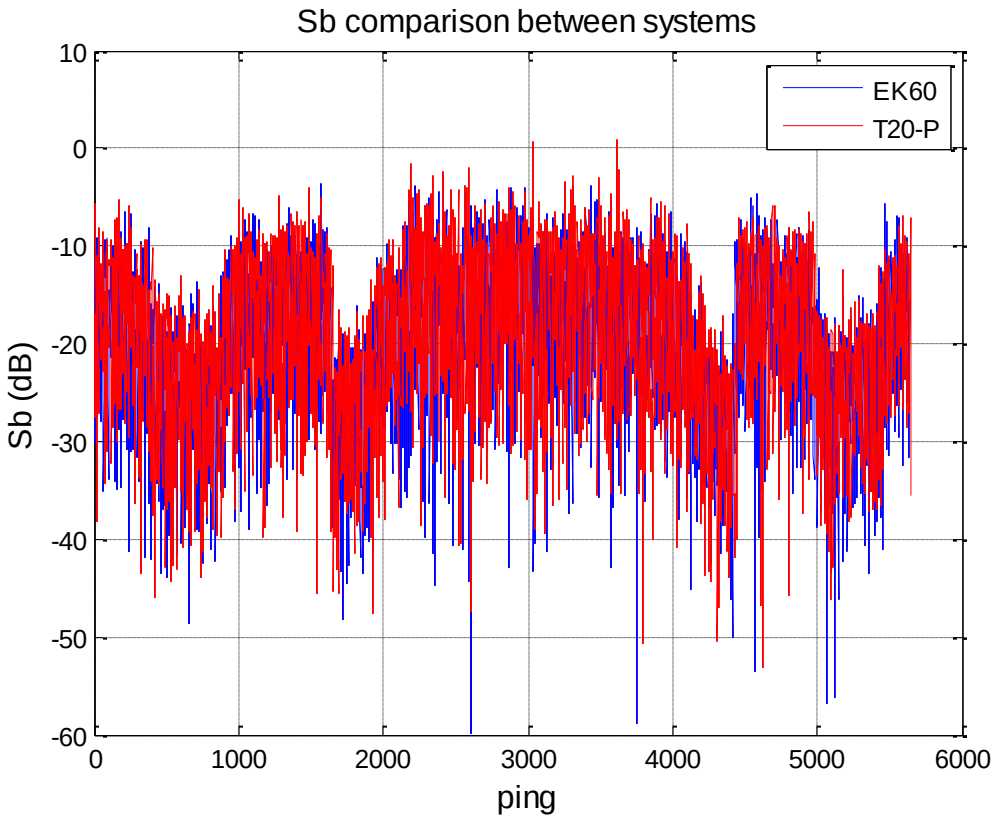

Figure 4.5 – Backscatter comparison between EK60 and T20-P beam 82 (steered to -45°, parallel to EK60 MRA), no averaging

Qualitative agreement is evident between the systems and significant overlap is clearly displayed. Acoustic backscatter measurements are stochastic in nature, and each measurement is the result of a sequence of random processes that are affected by several factors. The dominating factor is the

random nature of the seafloor scattering [11]. Separate clusters of 40 pings (not a running average) were averaged for each system to produce a more concrete comparison. The result of this averaging is displayed in Figure 4.6.

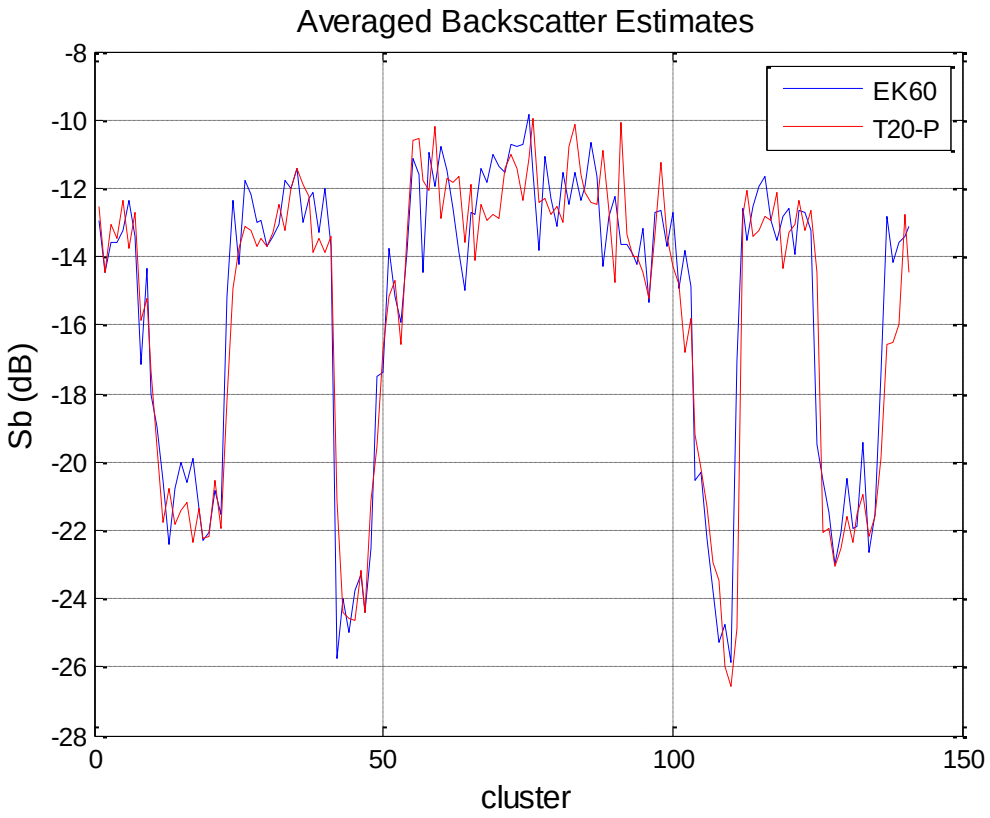

Figure 4.6 – Averaged backscatter estimates between EK60 and T20-P, 40 ping clusters

Qualitative agreement is clearly evident between the two systems. Figure 4.7 shows a close up of clusters 25 through 40, and this Figure outlines the agreement to the 95% confidence interval. The error bound for each system was calculated from equations 4.3 and 4.4,

$$Ss_{upper} = 10log_{10}(10^{\frac{meanSs}{10}} + \frac{1.96\sigma}{\sqrt{n}}) \quad (4.3)$$

$$Ss_{lower} = 10log_{10}(10^{\frac{meanSs}{10}} - \frac{1.96\sigma}{\sqrt{n}}) \quad (4.4)$$

Where *meanSs* is the average *Ss*, σ is the standard deviation, and *n* is the 40 ping population.

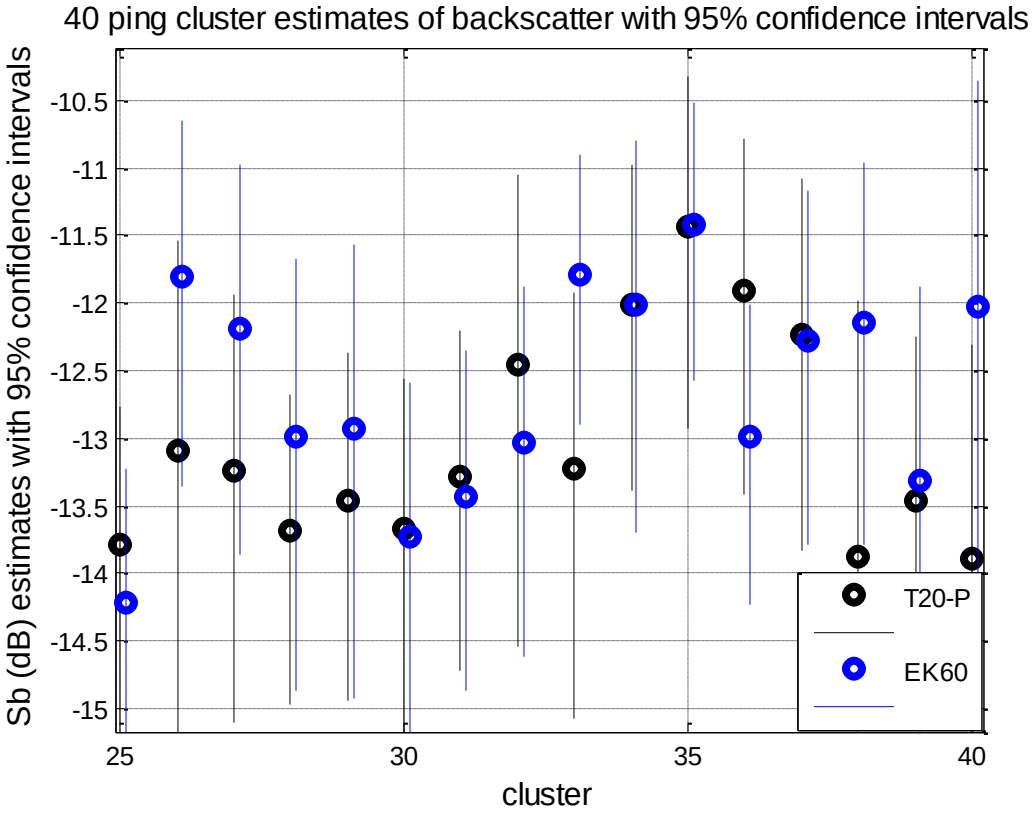

Figure 4.7 – Zoomed view of field data error estimates

One can see from Figure 4.7 that the 95% confidence limit from each system extends by roughly three dB, with almost 2.5 dB of overlap. A linear relation between the seabed backscatter estimates from the EK60 SBES and the T20-P MBES presents itself when the data from each system is compared independently of cluster number. This relation is illustrated by Figure 4.8.

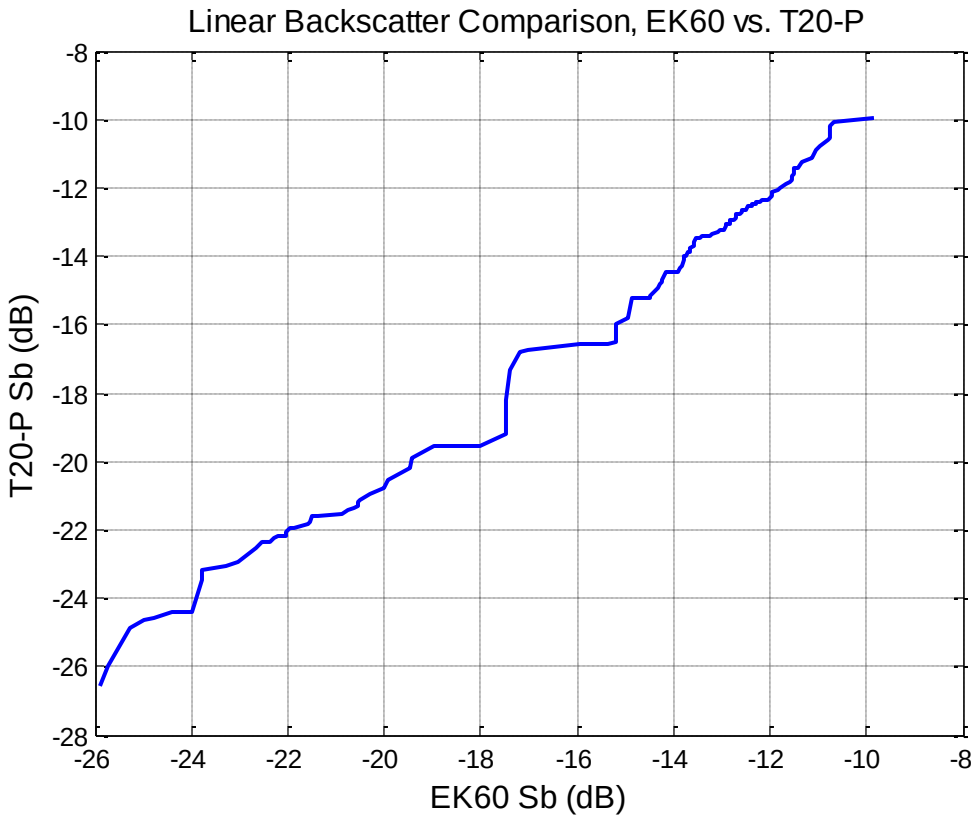

4.8 – Linear comparison of seabed backscatter estimates between EK60, T20-P

The KS-test was used again to investigate whether the field data from each system came from the same distribution. This is expected if each system truly surveyed over the same patch of seabed. Figure 4.9 shows the averaged cluster data and the associated P values for each cluster. If the P value is well above 0.05 then it is likely that the data between the two systems came from the same distribution.

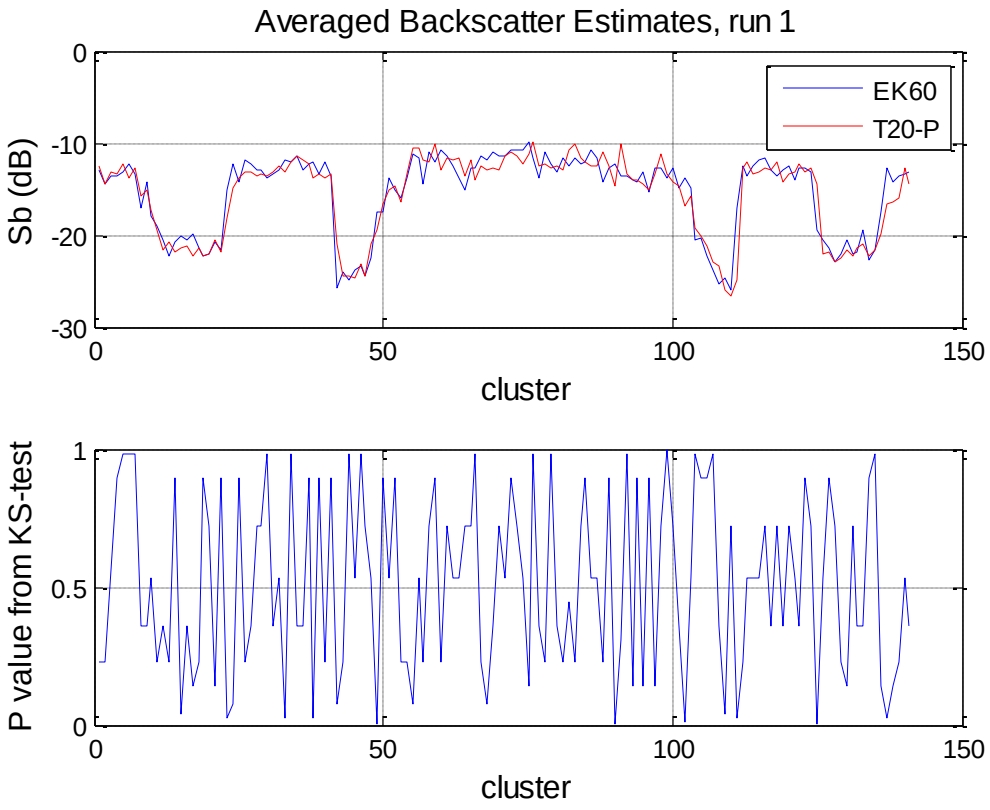

Figure 4.9 – Field data KS-test results

One can see that the P values are all above 0.05, leading one to believe that the data and results from each sonar system came from the same distribution.

At this point, the results show sufficient agreement between the two systems, suggesting that the calibration values determined from the tank experiment for the MBES were executed properly. If that is the case, then the entirety of the tank calibration curve should be applied to the MBES data to produce calibrated angle-dependant backscatter for the entire swath instead of just a single beam. This was done, taking care to use the correct limiting case of

area for each beam [19], and the results are presented in Figure 4.10 for clusters 15, 30, 45, and 60.

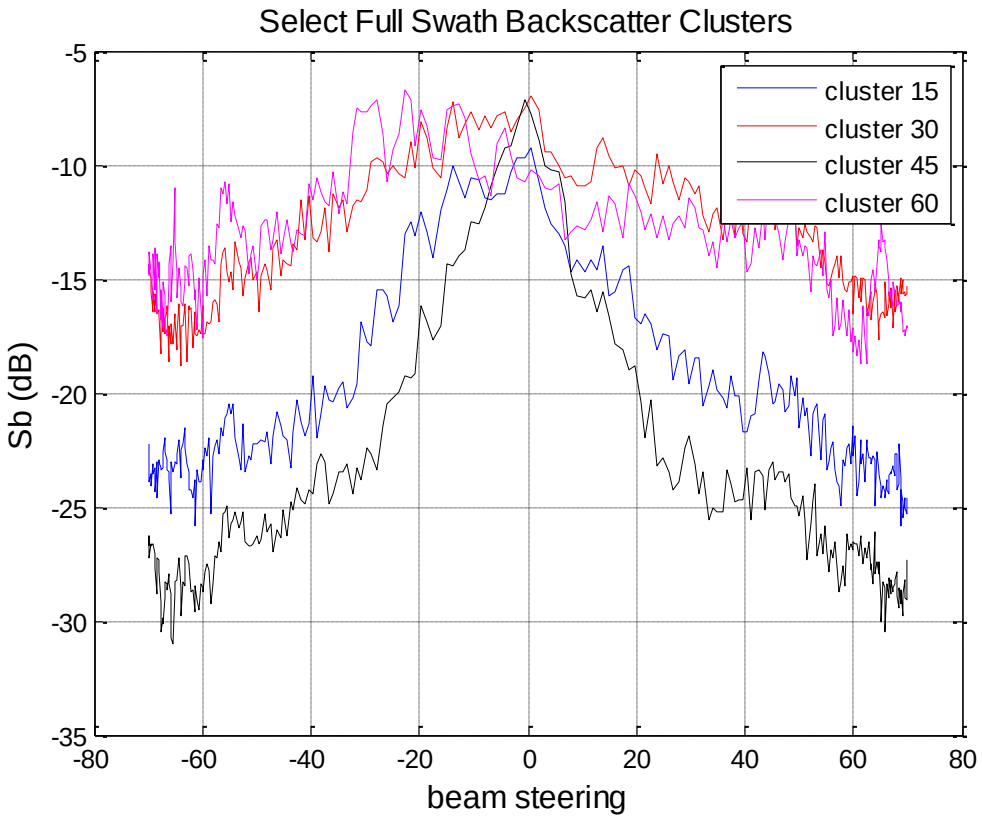

Figure 4.10 – Full swath backscatter estimates over certain locations

Figure 4.9 shows the backscatter values for the entire swath (for every beam) over changing sections of seabed. The backscatter was calculated using equation 3.10, taking care to use the proper beam footprint computation. The beam footprint was calculated using equation 3.4 near normal incidence, and equation 4.1 near oblique incidence. Near normal incidence, the beam footprint is limited by the beam-width, and near oblique incidence the beam footprint is limited by the pulse-length. A conservative approach to ensure that the correct

limiting factor was considered required calculating the area from both equations and using the smaller final value. While the noise in the backscatter estimates near the edges of the swath may present some difficulty in resolving slight differences between similar seabed materials, one can be confident in the general trend of each location. Clusters 15, 30, 45, and 60 were selected because they are clearly representative of different bottom types. These bottom types are known from separate efforts of the NEWBEX project that included sediment sampling and ground-truthing. Figure 4.11 shows thumbnail images of the bottom type representative of these ping clusters.

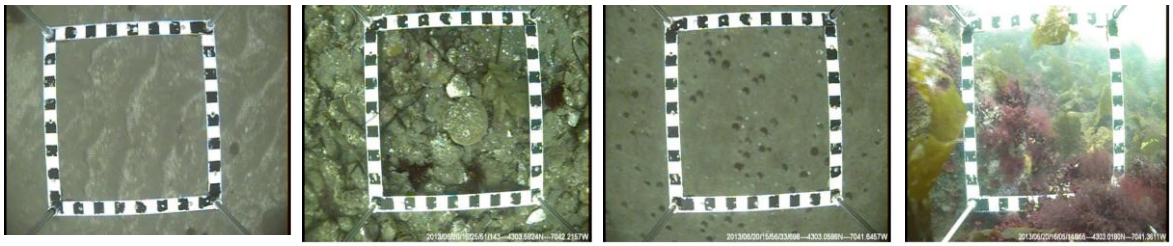

Cluster 15 Cluster 30 Cluster 45 Cluster 60

Figure 4.11 – Seabed characterization over clusters 15, 30, 45, 60 from NEWBEX standard line

The seabed around cluster 15 is characterized by sand waves and mega-ripples. The sediment in this area is known to be poorly to moderately sorted, and slightly granular to granular medium sands. The seabed around cluster 30 is predominantly composed of very poorly sorted to poorly sorted pebble gravels. The seabed around cluster 45 included slightly pebbly fine sands. Cluster 60 was representative of bedrock outcroppings, and piles of cobble. The area around cluster 60 is generally dominated by heavily vegetated rocky substrates.

The locations of these clusters along the line are displayed in Figure 4.12. Point B corresponds to cluster 15, point C corresponds to cluster 30, point F corresponds to cluster 45, and point G corresponds to cluster 60.

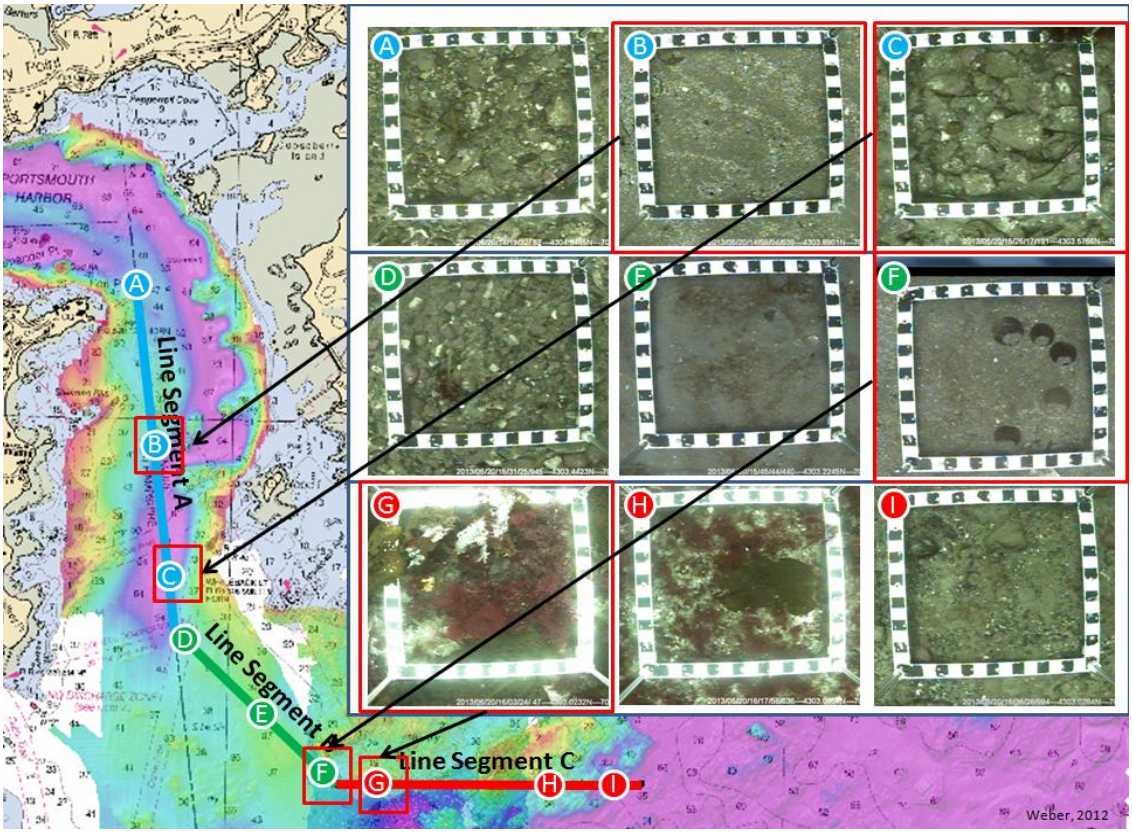

4.12 – Ping cluster locations along the standard NEWBEX survey line

The ground-truth data supports the angle dependant backscatter that was calculated and presented in Figure 4.10. Point F (cluster 45) is classified as fine sand and this location displays the lower backscatter when compared to a harder target like the bedrock at point G (cluster 60). Additional assurance is provided when one notes that the APL model included in Figure 4.3 agrees well with the backscatter calculated in Figure 4.10, and the simple seabed characterizations

displayed in Figure 4.11, and Figure 4.12. For example, At 45° cluster 15 reports backscatter of roughly -22 dB, and the APL model describes this as medium sand which is in agreement with the NEWBEX provided seafloor characterization of granular medium sand, described by Figure 4.11.

CHAPTER 5

CONCLUSIONS

5.1 – Conclusions and Remarks

The goal of this work was to develop a novel, simple and efficient methodology for calibrating MBES using an extended calibration target that replicates the morphology of the seafloor instead of using the typical reference sphere targets. Multi-beam echo-sounders (MBES) are becoming more frequent in seafloor mapping applications as well as fisheries and habitat mapping endeavors. Intensity calibrations are of significant importance with regard to increasing the utility of MBES backscatter measurements. Intensity calibration measurements in a tank with standard reference spheres can produce excellent results, but the amount of time required to complete such measurements is often prohibitively large. While split-beam echo-sounders (SBES) are able to be calibrated relatively easily with the tungsten-carbide (WC) reference spheres, it is significantly more difficult to conduct the same calibration on a MBES because these systems lack the split-beam capability required to precisely locate a point target within a beam. An alternative calibration method has been presented here. The calibration coefficient is a “catch-all” beam dependent value

determined from the sonar equation, and is used with regard to intensity calibrations.

The intensity calibration methodology for MBES proposed here employs an extended surface target comprised of randomly oriented “jack-chain” links. This new calibration approach was tested in the fresh water tank of the University of New Hampshire, demonstrating that it is a potential candidate for alternative intensity calibration methods. A more easily calibrated 200 kHz SIMRAD EK60 SBES was used to acoustically characterize this extended surface target in order to investigate any angular and range dependant backscatter. No relation was found to exist between the angle of incidence and the calculated *Ss* for the target. Similarly, the calculated *Ss* were found to be largely independent of measurement range to the target.

Once the chain target was acoustically characterized and the backscatter characteristics were made clear, then the target could be used for an in tank MBES intensity calibration. The MBES system that was calibrated in the tank with the chain target was a 200 kHz Reson T20-P. The backscatter from the chain target was analyzed and found to originate from a Rayleigh distribution. This is an attractive characteristic for an extended target meant to simulate the seafloor. Calibration comparison measurements unique to the T20-P MBES were recorded for select clusters of beams with a standard 38.1 mm tungsten carbide reference sphere. The sphere was measured on axis and provided a way to check the calibration curve generated from the chain target at particular points in the swath.

Agreement between the calibration values determined from the chain target and the WC sphere was satisfactory, and both systems were brought to sea for a field experiment. The calibration produced in the tank was meant to be applied to a set of field data to produce calibrated seabed backscatter estimates over a previously characterized patch of seabed, or 'standard line'. Seabed backscatter estimates (*Sb*) should match between both systems once the tank calibration is applied to the MBES. Both the EK60 SBES and T20-P MBES were mounted to the ram of the UNH CCOM/JHC owned and operated R/V Coastal Surveyor. The systems made use of a trigger controller to regulate the ping rates of each system and a survey was run over a standard line in Portsmouth Harbor, Portsmouth, NH. Seabed backscatter results agree at the 95% confidence interval and the data from each system was shown to come from the same underlying distributions, thus confirming that the goal of this work has been achieved. Calibrated intensity measurements have successfully been attained, and were achieved in a condensed amount of time than previous intensity calibration methods could be completed. One calibration sweep was all that was required for this work. While the results of this work are promising, there are some limitations to this proposed calibration methodology that must be addressed. As it stands, this calibration method requires a custom built extended target, and a test tank facility. Meeting these requirements may be unrealistic for some users.

Further research should include considerations into an automated dynamic agitator for the chain target during any tank calibration work. The chain

target was manually moved back and forth, approximately 10 cm/s to provide an adequate number of independent realizations of the target. This type of manual movement, while sufficient for the purposes of this experiment lacks a precise quantifiable measurement of movement. Additional further research could be done to apply this extended target calibration method to field calibrations. Present field calibrations use the same reference sphere targets that were described in this thesis [14]. The same difficulties that were present in a controlled test tank environment exist for field calibrations as well. A sphere must be suspended from flexible rods fixed to a vessel and moved along beams directed toward the seabed in both the alongship and athwartship directions. This is done all while the sonar is mounted to the hull, or ram of the vessel. It may be possible to implement a field calibration version of this extended target to ease the complications of calibrating on a vessel. A smaller version of the jack-chain extended target could be suspended from these flexible rods, and positioned under the vessel in a manner where it would be parallel to a flat seafloor. If the MBES were fixed to a mount that could precisely rotate the system around the roll axis of the vessel, then a similar calibration sweep could be completed.

REFERENCES

LIST OF REFERENCES

[1] J.S.Bendat, A.G. Piersol, “Random Data: Analysis and Measurement Procedures”, Third Edition, Wiley Publishing, 2000

[2] C. Brown, P. Blondel, “Developments in the application of multibeam sonar backscatter for seafloor habitat mapping”, Applied Acoustics 70 (2009) 1242-1247

[3] D. Chu, “TS Package”, ComputeSolidElasticSphereTS Matlab GUI, NOAA

[4] Foote, K.G., et al. “Calibration of Acoustic Instruments for Fish Density Estimation: A Practical Guide”, No. 144. International Council for the Exploration of the Sea, 1987

[5] Foote, K. G., et al. “Protocols for Calibrating Multibeam Sonar”, the Journal of the Acoustical Society of America, 117, 2005

[6] Francois, Garrison, *Calculation of absorption of sound in seawater*, 1982 model, [online], Available: http://resource.npl.co.uk/acoustics/techguides/seaabsorption/

[7]S.F. Greenaway, “Linearity Tests of A Multibeam Echosounder”, MS Thesis, Center for Ocean and Coastal Mapping/Joint Hydrographic Center, University of New Hampshire, 2010

[8] S.F. Greenaway and T.C. Weber, “Test Methodology for Evaluation of Linearity of Multibeam Echosounder Backscatter Performance”, Proc. MTS/IEEE Oceans 2010 Conf., Sep. 20-23, Seattle, WA

[9] E. Hammerstad, EM Technical Note, “Backscattering and Seabed Image Reflectivity”, 2000

[10] J. Heaton, T. Weber, G. Rice, X. Lurton, “Testing of an extended target for use in high frequency sonar calibration”, Conference Proceedings, J. Acoust. Soc. Am., Vol. 133, No. 5, Pt. 2, May 2013

[11] D. R. Jackson, M. D. Richardson, “High Frequency Seafloor Acoustics”, Springer Publishing, 2007

[12] L.E. Kinsler, A.R. Frey, A.B. Coppens, and J.V. Sanders, “Fundamentals of Acoustics,” 4th ed., Wiley, New York, 2000

[13] J.C. Lanzoni and T.C. Weber, “Calibration of multibeam echo sounders: a comparison between two methodologies”, Proc. of Meetings on Acoustics, vol.17, pp.070040, Dec. 2012.

[14] J.C. Lanzoni, T.C. Weber, “High-resolution Calibration of a Multibeam Echo Sounder”, Proc. MTS/IEEE Oceans 2010 Conf., Sep. 20-23, Seattle, WA

[15] J. C. Lanzoni, T. C. Weber, “A Method for Field Calibration of a Multibeam Echo Sounder”, MS Thesis, Center for Ocean and Coastal Mapping/Joint Hydrographic Center, University of New Hampshire, 2011

[16] J.C. Lanzoni, T.C. Weber, “Reson Seabat 7125 Multibeam Sonar System Calibration”, Center for Coastal and Ocean Mapping/Joint Hydrographic Center, University of New Hampshire, 2013

[17] X. Lurton, “An Introduction to Underwater Acoustics”, Praxis Publishing, 2010

[18] X. Lurton, “Swath Bathymetry Using Phase Difference: Theoretical Analysis of Acoustical Measurement Precision”, IEEE Journal of Ocean Engineering, Vol. 25, No. 3, 2000

[19] X. Lurton, S. Dugelay, J.M. Augustin, “Analysis of multibeam echo-sounder signals from the deep seafloor”, IEEE, 0-7803-2056-5, 1994

[20] A.P. Lyons, D.A. Abraham, “Statistical characterization of high-frequency shallow-water seafloor backscatter”, J. Acoust. Soc. Am. 106, September 1999

[21] I. Parnum, A. Gavrilov, “High-frequency multibeam echo-sounder measurements of seafloor backscatter in shallow water: Part 1 – Data acquisition and processing”, International Journal of the Society for Underwater Technology, Vol. 30, No. 1, pp 3-12, 2011

[22] Rossing, Moore, Wheeler, “The Science of Sound”, 3rd edition, Addison Wesley Publishing, 2002

[23] J. Simmonds, D. MacLennan, “Fisheries Acoustics: Theory and Practice”, second edition, Blackwell Publishing, 2005

[24] W.T. Thomson, M.D. Dahleh, “Theory of Vibration with Applications”, 5th Edition, Prentice Hall Publishing, 1998

[25] R. Towler, *readEKRaw EK/ES60 ME/MS 70 Matlab toolkit*, NOAA Alaska Fisheries Science Center, [Online], Available: http://www.hydroacoustics.net/viewtopic.php?f=36&t=131&start=0

[26] R.J. Urick, “Principles of Underwater Sound,” 3rd ed., McGraw–Hill, New York, 1998

[27] B. Welton, “Backscatter Measurement Variation between NOAA’s Reson 7125 Multibeams and a Method for a Relative Field Ca libration between Systems”, MS Thesis, University of New Hampshire, 2014